Index

North Sea FLOW Measurement Workshop

Paper 7.1

First Ever Complete Evaluation of a Multiphase Flow Meter in SAGD and Demonstration of the Performance Against Conventional Equipment

Bruno Pinguet
Schlumberger

Fernando Gaviria
SUNCOR Energy

Laurie Kemp
SUNCOR Energy

John Graham
SUNCOR Energy

Cal Coulder
SUNCOR Energy

Carlos Damas
Schlumberger

Karima Ben Relem
Schlumberger

TÜV SÜD

nel technology for life

First Ever Complete Evaluation of a Multiphase Flow Meter in SAGD and Demonstration of the Performance Against Conventional Equipment

Bruno PINGUET, Schlumberger
Fernando GAVIRIA, Laurie KEMP, John GRAHAM and Cal COULDER, SUNCOR Energy
Carlos DAMAS and Karima BEN RELEM, Schlumberger

1 INTRODUCTION

Suncor and Schlumberger have been working over several years to establish the performance of multiphase flow meters and determine the accuracy and reliability of flow-testing equipment for thermal heavy oil production, the first test was carried out in 2007. The test marked the first successful application of multiphase flow metering in Canadian thermal recovery operations.

The initial introduction leads to selection of a well for its dynamic conditions and production history factors such as flowrate, line pressure, line temperature, and fluid properties and allowed the connection of the MPFM (the Vx) in series with an existing test separator.

The multiphase initial objectives were to measure the well's oil, water, steam, and gas flowrates, understand the well's SAGD dynamics, and the impact of changes in ESP frequency to experience different production conditions, including line pressure, flowrates, phase fractions and ratios, i.e., Water/Liquid Ratio (WLR). Finally, to study the Vx's sensitivity and performance against a valid reference by defining the results for stability, dynamic response, repeatability and reproducibility. This leads to several papers presented in different conferences (Ref [1-3], and in the meantime to work closer to define what should be the optimal test of a cluster to have a full understanding of the technology and the potential for permanent installation.

In 2009, a second and more advanced field trial was initiated. A pad was selected as the location for this field test due to the large number of good producing wells and ideal set up of the conventional equipment. The MPFM was connected in series with the conventional test separator and the test was divided into three stages to fully evaluate the safety, reliability, accuracy, and advantages of the MPFM over the conventional test separator equipment.
During the first stage, 9 wells were tested during the months of October and December 2009, ensuring that the MPFM was challenged against the full range of operating conditions of the SAGD wells. During two months of extensive well testing and fluid sampling, no safety incidents were encountered and the MPFM reported well production rates continuously and without any performance degradation even during the extreme cold ambient temperatures recorded at the well site.
To demonstrate the reproducibility of the flow measurements using the MPFM, a second stage was completed, this time shortening the flow period from 12 hours to 6 hours and then be able to demonstrate the capability to do more well tests per month per well with the same quality data. Then, with the Vx meter only, the data of the 12 hours testing were reprocessed for 4 hours showing a very good consistency in the results with the 12 hours test.
Results, from the second stage of the test confirmed that the data is identical for a 12 hours test versus the 6-hour test versus the 4 hours test and has very good repeatability and prove the robustness and independence of the flow regime. These results seem to reveal that testing for shorter period of time and more frequently gives more information and is likely preferred to be able to optimize production.
A third phase more dedicated to optimization potential and the impact of changing chokes, steam injected rates and other numerous parameters was done but it will be only briefly mentioned in this paper.

2 PROBLEM AND PROPOSED SOLUTION

The SAGD process presents one of the most challenging environments for flow rate metering in the industry. Produced fluids are often characterized by unstable flow regimes, high temperatures, emulsified foamy oil, as well as the presence of H2S and abrasive sand particles. As such, the capture of good data is extremely difficult.

Timely and accurate well production data is required for the validation process of the reservoir model and for confirmation of production predictions. Additionally, the oil company could potentially utilize this valuable information to adjust the operation for optimum performance. Currently, the industry attempts to meet this need using “test separators”, which employ the basic principle of gravity of the various phases that produce through the wellhead. Additional standard equipment, such as a water-cut meter, Coriolis, and orifice plate technologies are then employed to obtain the measurements.

However, it is well known that there are many issues, which compromise the accuracy and utility of the data retrieved by this conventional equipment. First, as oil and water density contrast is very low, the gravitation process is not effective and do not allow for proper separation of the gas and liquid phases. Second, there are issues regarding the proper measurement of the mix of steam vs. natural gas, of oil vs. water, and with known errors from gas entrainment within the liquid lines. Lastly, because many wellheads share a single test separator, flow measurements from each individual well can only be periodically obtained. Some additional backpressure may also affect the estimated well production.
These factors lead to a limited understanding of each well’s performance and a negligible capability for optimization. Thus, it is desired to find a technology that could replace the separator system with a real time and accurate metering system.

The primary goal of this collaboration is to develop production techniques that will improve the productivity and recovery factors of viscous oil sand reservoirs in Canada, starting with Suncor’s Firebag Asset. Firebag is located 140 kilometers northeast of Fort McMurray, Alberta, Canada (Figure 1). The first barrel of bitumen produced from this operation was processed in January 2004.

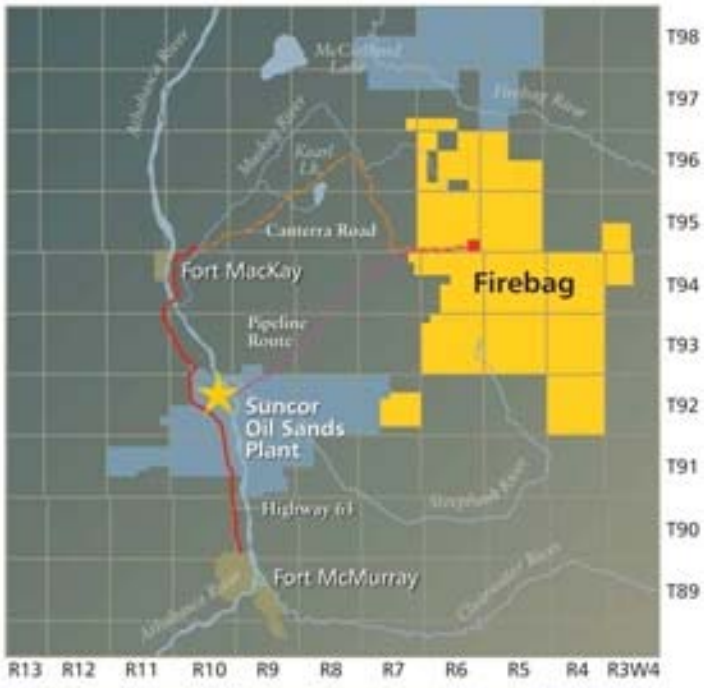

Figure 1: Field location

With a viscosity of millions of centipoises [cP], the oil is not producible through ordinary cold production practices. Rather, the bitumen is extracted via an advanced and complicated recovery technique known to the industry as SAGD (Steam Assisted, Gravity Driven).

From this basis, a collaborative project plan was developed with the mission to bring optimized workflows and new technologies to Firebag that will achieve a reduction in Steam-to-Oil (SOR) of at least 0.50 while reducing the environmental footprint. The project was planned to complete three phases, each with a deliverable during a calendar year:

- Phase One: Enable Firebag to have real-time accurate production flow data
- Phase Two: Working with this data, enable the operation with advanced monitoring, automation, and optimization systems
- Phase Three: Once optimization techniques are available, add the capability for active/adaptive completion technologies (e.g. steam injection control)

Figure 2: Field Operation and Equipment Proposed

Only after completion of the phase#1 successfully, the project could advance to Phase 2 of the aforementioned mission to significantly reduce Firebag's SOR and environmental impact. To answer all different issues rose above and if this is possible, the solution will be based on a system without any separation. This paper presents the fieldwork that was conducted during Q4, 2009 and completes the deliverable for Phase One.

It is proposed to replace the centralized test separator system with a Multiphase Flow Meter (MPFM), shared either by many wells or ideally at each wellhead for full real time capability. Such a set up could provide a step change in performance and a reduction in surface footprint. In addition, continuous well flow measurements could be used to optimize the artificial lift performance, maximize oil production, and improve the energy balance. If this present a step change in SAGD conditions, Vx technology has been already accepted in conventional field development. Approval for allocation in North Sea has been done (Norway through NPD, UK with DTI) or Gulf of Mexico (USA with MMS).

Schlumberger has successfully developed an advanced MPFM, based on the "Vx technology" and available as mobile unit (PhaseTester used for this test) and permanent unit

PhaseWatcher that may provide an ideal solution. Originally designed for challenging deep-water markets, this multiphase flowmeter has been used in hundreds of applications and has proven to be reliable and accurate. Over the past few years, this device has been introduced to the SAGD/Thermal environment via several field trials in Western Canada and Mexico. Because of these learning, many improvements (e.g. increasing the temperature rating) have since been commercialized.

3 PROPOSED SOLUTION

An overview on the basic operational principles of MPFM devices was given in 2008 at the World Heavy Oil Congress [2] and is partially reproduced below for convenience. At a minimum, all MPFM devices will output the oil, water, and gas flow rates at line conditions. These outputs are derived using either a physical or an empirical model. However, industry reports production at standard conditions and therefore the flow rates at line conditions need to be converted to standard condition using PVT correlations or more properly named "fluid behaviour model". Capturing this flow behaviour can be done by simply looking at few macro parameters: Volume factors (bo, bg, bw), Gas dissolved in Oil (Rst), Gas Dissolved in Water (Rwst), and the water phase condensation (rgwmp).

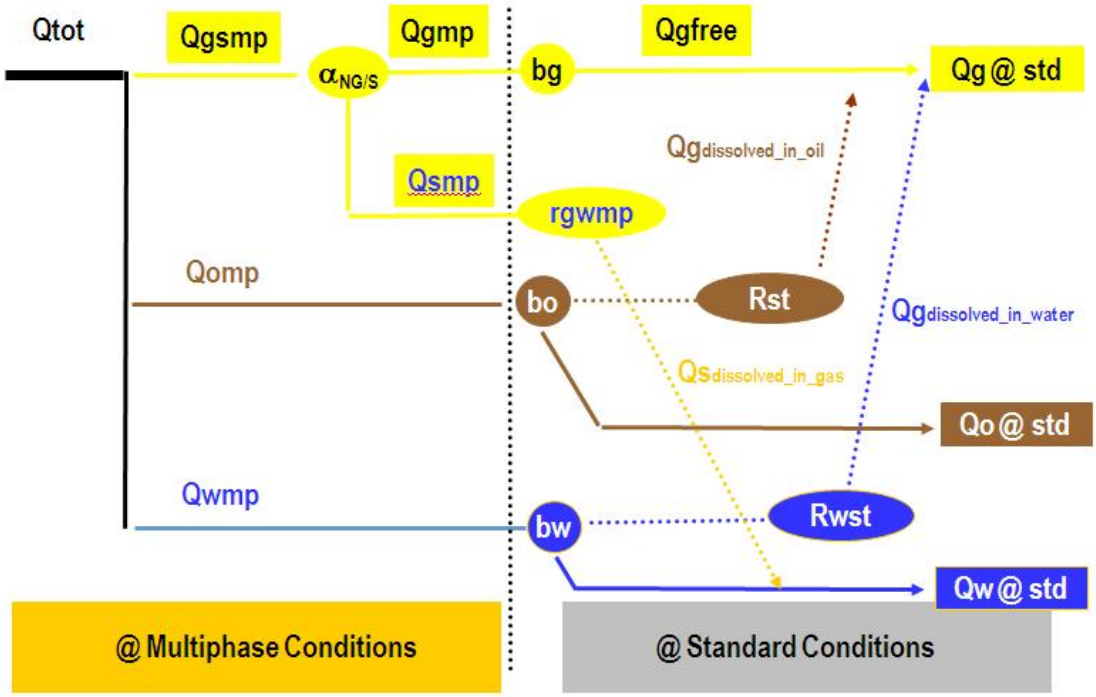

Figure 3: Field Operation and Equipment Proposed

Of course the knowledge of the density of each fluid at line conditions will be necessary and can be obtained based on the above parameters and the knowledge of the dead water and oil and specific gravity of the gas.

In the SAGD environment, it is a combination of a few simple and basic measurements done at the well site or through some laboratory analysis, or information available through a PVT report, which will be used to tune the EOS (usually build for a pad or a flied following the homogeneity of the reservoir). The combination of the accuracy of the representation of the mass or volume converted from line to standard conditions with the intrinsic accuracy of the multiphase flow meter (specific to each technology and then multiphase manufacturer) provides the global accuracy of the measurement of live effluent. The physical principle and model has been done by a review systematically of each implication to work in SAGD. This is the result of 10 years of focus and understanding in details of the Vx technology.

The Vx multiphase flowmeter (figure 4) contains three main modules:

- An advanced multiphase flow model of the fluid mechanics,
- A robust measurement of the total mass flow rate based on the well-known Venturi design, and differential pressure concept
- A robust fraction meter measurement based on established nuclear technology, to produce in real-time fraction measurement of oil. Water and gas without any separation and being not sensitive to the phase distribution (emulsion, foam, droplets flow, water contents...).

A detailed explanation of the specific data flow processing routine and various assumptions made within the Vx technology can be found in the referenced documents [2]. However, a summary is listed below for convenience:

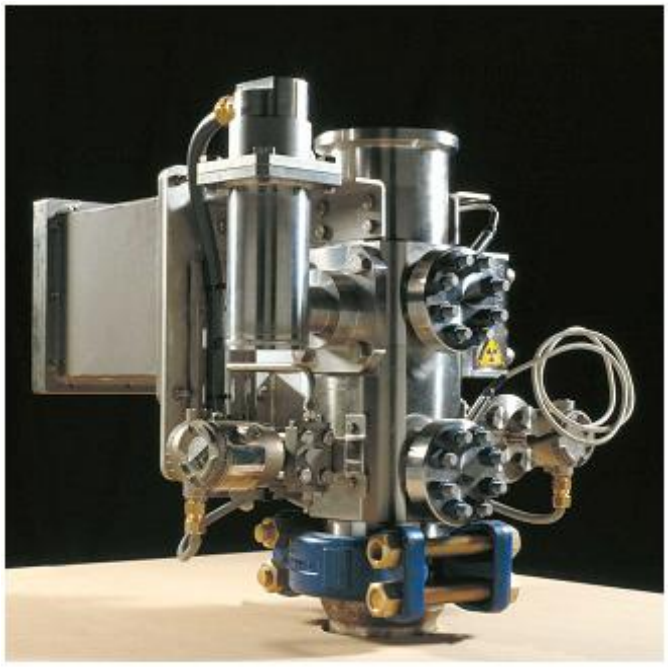

Figure 4: Field Operation and Equipment Proposed

Two basic measurements are made in the Venturi section:

- Differential pressure across the Venturi (ΔP), and
- A multi-energy gamma-ray fraction meter, which provides fraction of each constituent of the mixture (αo, αw, αg).

Additionally, there are sensors that measure process fluid pressure at the Venturi throat, fluid temperature upstream of the Venturi section, and ambient temperature.

It is essential here to mention some fundamentals of the fluids mechanics to be able to have an accurate multiphase flow meter in general. First, the flow is turbulent or chaotic and then it is necessary to have a system working at a frequency much higher than several 10th of Hz. Second, the different fraction measurement needs to be correlated; this means that from a recording time point of view all measurements should be done at the same time. Third, because the flow is turbulent then the timing is important and because the fluid is a live fluid then the acquisition should be done at the same space. Fourth, this recording should be done at the same pressure and temperature. With an example is easy to understand, if for example the water holdup was done in one place at a certain pressure and temperature or done

somewhere else at different pressure and temperature then the condensed water will be different and then the overall calculation of the water content could be either overestimated or underestimated,

The Vx technology is built on a few physical hypotheses: No slippage inside the liquid phase, a semi-empirical model of the gas-liquid slippage based on extensive research and experiences made at low pressures (from 1 to 30 bar) with immiscible fluid, and finally a model of a "shape factor" for multiphase environment.

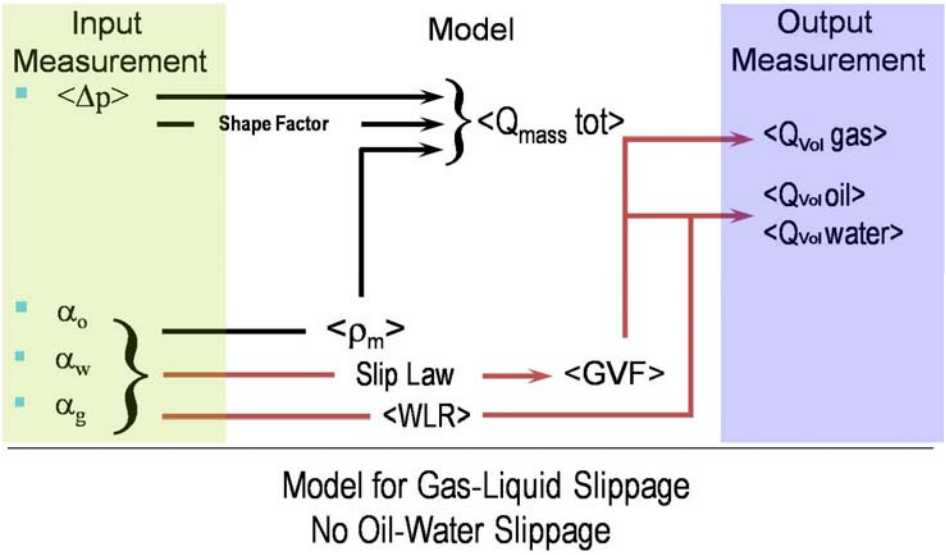

Figure 5: Field Operation and Equipment Proposed

Similar to the common dataflow for all MPFM devices, the specific Vx schematic is shown Figure 5. As already mentioned the volumetric flow rates at standard conditions are the main outputs and computed from the flow rates at line conditions using either a PVT software package or a correlation (as it is currently done for the separator).

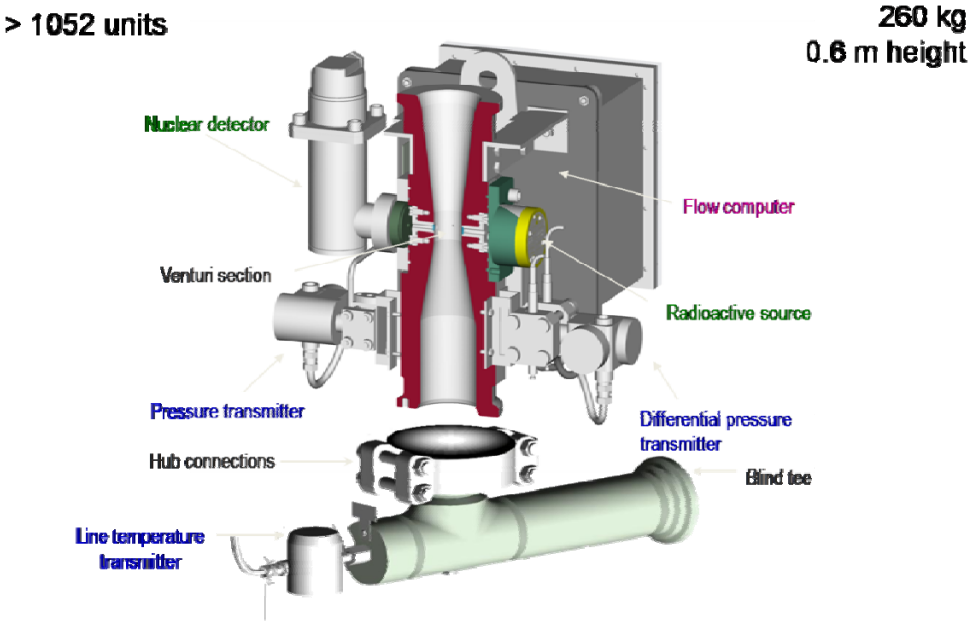

Figure 6: Field Operation and Equipment Proposed

The Vx technology is the simplest combination of sensor and technology available on the market today with only 4 sensors and none of them in direct contact with the fluid avoiding the high temperature stress.

An additional challenge for SAGD operations is to monitor at surface: Steam (i.e. Vapour of water), Natural Gas evolved from the Oil, Bitumen, and then Water (Liquid form). This means there are four phases versus the traditional three at line conditions. Therefore, it is necessary to use additional information to obtain this fourth phase measurement. The Vx device can provide four phase measurements and split the fractions of Steam and Natural Gas by using a dedicated Equation Of State (EOS) package based on the knowledge of the fluid properties. This allows keeping the multiphase flow meter design as simple as possible without additional sensors, cost, and maintenance program.

The Vx technology has a unique application within SAGD operations due to the use of a specific heating device, which allows the entire nuclear-based instrument to be kept at a specific temperature, and can handle any fluctuation of the fluid temperature passing through with minimum impact on the accuracy of the fraction measurement.

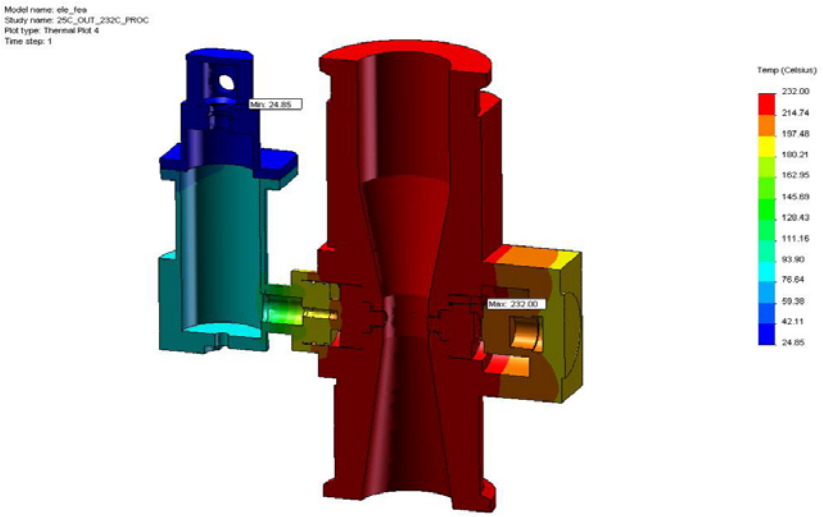

Figure 7: Field Operation and Equipment Proposed

Extensive testing has demonstrated that under the harsh conditions (no wind, ambient temperature at 25 degC, and flow temperature at 232 DegC) the sensor will not exceed 80-90 DegC in the worst conditions when the electronic has been designed to handle more than 100 degC in normal operation. In addition, The structural design of the Vx Multiphase Flow meters complies with the reference codes and standards of Canada or International.

The key points of the Vx Technology are summarized below:

- No Tuning Factor due to a proper understanding of the fluid mechanics
- No Separation by construction
- No Flow Calibration the measurement being based on physics principle
- No issues with Foams or Emulsions due to nucleonic technique of measurement
- Improve water detection and accurate BSW monitoring (either oil or water continuous phase)
- Continuous rate measurements
- No moving parts
- Different sizes: 29mm, 52mm, 88mm (100 – 150,000 bpd)

- Due to the Venturi principle used in the Vx technology an extremely low back pressure
- Compact solution (<300 kg, 2 feet tall)
- No Sensor in direct contact with the fluid
- Full sampling capabilities (optional)

The Figure 12 presents a comparison in footprint between the conventional Test Separator, the Vx PhaseTester (periodic applications) and the Vx PhaseWatcher (permanent installations).

Figure 8: Field Operation and Equipment Proposed

4 MOTIVATION FOR A SECOND TRIAL Vx TEST

As described above, the Vx technology was used for the first time in SAGD in 2007 at the Suncor Firebag Project. This represented the first introduction of the technology to SAGD environments and was published in different conferences around the world in 2008 (Ref. [1-3]).

The decision to initiate a second Vx field trial with Suncor and finalize the introduction of Vx for SAGD was a result of the completion of several new improvements of the test separator and a tighter focus on the metrological performance comparison versus 2007. Additionally, the first Vx Trial in 2007 was specific to a single well in the SAGD pad. The second trial is covering a much wider range of wells and operating conditions in order to prove the accuracy and reliability of the Vx flowmeter in all conditions encountered during a SAGD project operation.

Schlumberger has been working with another operator throughout 2008. During this particular project, extensive testing was done and both parties were able to challenge the Vx Technology and conventional equipment to review how a multiphase flow meter could be becoming a reference measurement in SAGD operations (Ref [4]).

The main improvements after the 2007 Vx trial are summarized below:

- Design and implementation of a sampling equipment to collect Gas-Steam samples at line conditions and be capable to measure the steam and natural gas ratio
- Design and implementation of a sampling equipment to collect liquid samples at line conditions to be used as reference WLR measurement due to lack of robust conventional sensor for SAGD conditions
- A comprehensive review of the fluid properties behavior, development of the full PVT to handle either 3 or 4 phase in SAGD at the well site (Oil, Natural Gas, Vapor of water, Water)
- A complete review with Engineering center of the future improvement to do in the commercial software to be SAGD compliant (fluid behaviour and 4th phase compliant)
- Starting the process of an entire review by DNV of the equipment for SAGD operation as a permanent multiphase flow meter
- Improvement of the Vx WLR measurement at line conditions through a new algorithmic process
- A proper understanding and a written procedure to handle dead sample to provide the Reference
- An update of the EOS generator (PVT Pro) for SAGD field and taking into account the steam ratio
- Validation of the Vx measurement at higher temperature then 190 DegC
- Validation of the Vx measurement in environment with water and high H2S content in SAGD
- Demonstration of the good accuracy in PCP conditions
- Review of the performance in details of the multiphase flow meter (flow rates) versus conventional equipment and definition of the strong and weaker point of the multiphase solution versus conventional equipment (Ref. [4]).
- Use in unstable conditions to capture the flow dynamic and also in stable production to see the same performance than the separator
- Use in the large concentration of CO2 (> 9%)
- Sensitivity analysis and what should be the maintenance program to define to keep the same level of uncertainty in permanent application through the Vx advisor software.

Based on this significant list of technical improvements, it was agreed by both parties that performing a second Vx trial at Firebag will bring value to both companies and would help reaffirm the capabilities of the Vx technology for SAGD conditions.

4.1 Qualifications & test Objectives

In order to qualify the Vx Technology for SAGD operation, a series of field tests were conducted at Suncor's Firebag asset during Q4, 2009. The Vx Multiphase flow meter was connected in series with the conventional test separator and the test was divided into three stages with review of the performance at the end of each stage before progressing to next stage and described as follows:

Stage #1: Benchmark (Vx vs. Test Separator)
This first stage will be to compare the performance of the Vx MPFM against the currently utilized test separator.

1. Demonstrate Vx installation procedure and set up process
2. Demonstrate gas and multiphase sampling capability
3. Benchmark Meet or exceed all metrics currently employed by the operator
    1. Accuracy & repeatability of all flow measurements (expected to be within 5%)
    2. Frequency of test duration (12 hrs or less)
    3. Capability to test each well head at least twice per week
    4. Capability to derive Gas/oil Ratio (GOR) and Steam/Oil Ratio (SOR)

5. No failures or reliability issues
6. Safety

Stage #2: Advanced Vx Capabilities
This stage focus on additional capabilities versus current test separator.

1. Evaluate shorter test duration cycles (e.g. 4 hours vs. the current separator 12 hour cycle)
2. Demonstrate accurate measurements of both natural gas and water vapor

Stage#3: Optimization Techniques
This last stage focuses on gaining an insight into the potential for optimization, which will be the basis for the next two phases of the project.

1. Evaluate Vx dynamic response capabilities
2. Explore the potential for production optimization

4.2 Installation

The Pad which was selected for this field test due was upgraded lately and has a large number of good producing wells and ideal set up of the conventional equipment. Wells were producing either naturally or by artificial lift (ESP pump). The presence of a 10" by-pass manifold on the pad production line and the capability to easily modify the current installation by implementing two 8" spools to connect to the Vx meter was a non-negligible factor. The metrological equipment of this PAD had also been totally updated or reviewed before this test.

For commodity and cost savings, the Vx mobile unit ("PhaseTester") was used. However, it should be noted that the permanent unit ("PhaseWatcher") utilizes the same technology but it is lighter and more compact. The only difference between these two tools is the mobility. For the duration of the three-stage program, 9 of 11 wells were tested. The remaining two other wells were not accessible or not producing at that time.

Figure 9: Field Operation and Equipment Proposed

The Vx meter was connected downstream of the test separator due to the design. Well effluents exiting from the test separator were recombined before flowing to the MPFM.

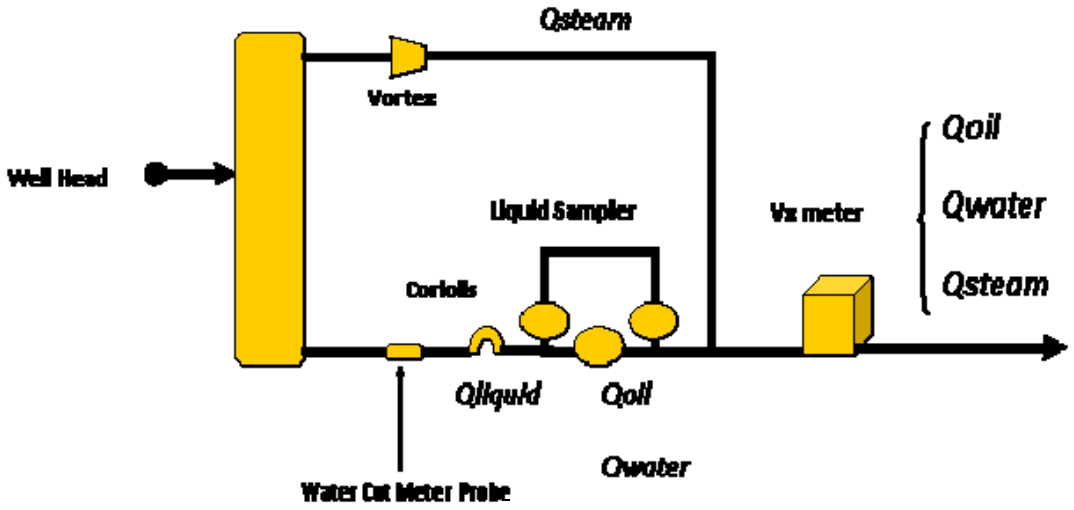

Figure 10: Field Operation and Equipment Proposed

The schematic (Fig. 10) illustrates the basic set up of the test separator and associated reference meters. As the two streams exit the separator, the gaseous phase is routed through a vortex meter in order to measure steam flow and is recombined with the fluid flow later. The liquid flows at the bottom first through water cut meter probe, then through a Coriolis meter and liquid sampler bypass.

It should be noted that the flowrate measurements accuracy could be affected due to some limitation associated with several required assumptions (listed below), but also intrinsic errors cause by various sensors. As conclusion the separator results should not be considered to be exact (like any others measurements) but the most correct one if the hypothesis and equipment are fully within their working envelope.

Assumptions or additional data required for the current test separator system:

- Gas line is assumed to be only water vapor (no natural gas) leading to a production of 2% more of condensed water in average
- Salinity input is required to get water-cut measurement due to the microwave technology used and this equipment seems to be very sensitive to the salinity parameter
- No gas is assumed to be passing through the liquid line
- No liquid is assumed to be passing through the gas line
- A Liquid Sampler by-pass is set to verify Water-cut Meter, and in average through the data obtained it is more than 8% absolute error that can be noted with in some cases more than 20% absolute deviations.

4.3 Multiphase Meter Settings

The setting of the multiphase flowmeter is based on a few input parameters that are essentially associated with the nuclear fraction measurement device. The mass attenuation parameter is an intrinsic parameter of the fluid composition and it is used to calculate each phase fraction flowing through the venturi throat. It is strongly recommended in SAGD operation that the mass attenuation determination for the first commissioning is performed in the base (more control conditions) and then confirmed on site. However, it is possible to get these intrinsic properties from the fluid composition. The mass attenuation is constant whatever the temperature and pressure. Moreover, it is not dependent of the long chain of alkans and then a composition in C5+ or C9+ is good enough.

Once a liquid sample is retrieved, the oil is separated from the water and processed in order to obtain the most accurate mass attenuation data for each phase. From this sample, the specific gas, oil, and water points are utilized to set the meter. Then when the commissioning (i.e., configuration file downloaded to the meter) is finished, then a map as illustrated below is available. Each point of the triangle represents 100% of each phase, and then any mix of the 3 phases will be within the triangle defined by the APEXES of oil, water, and gas (Figure xx).

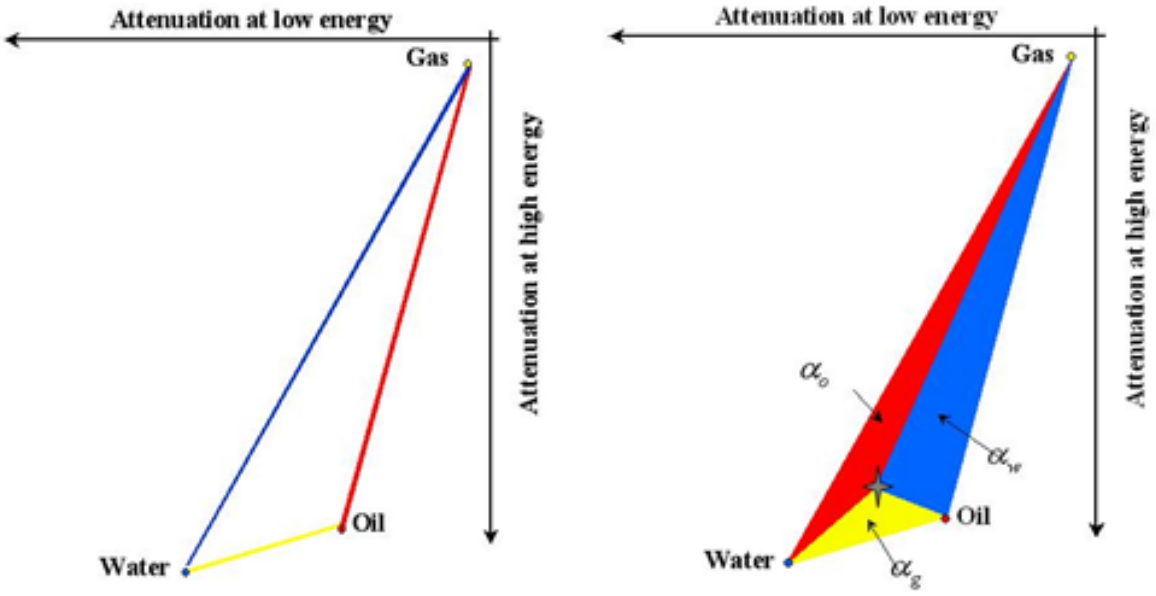

Figure 11: Field Operation and Equipment Proposed

Based on the composition obtained from Suncor (via Hysis) a VxFluidsID (i.e. fluid behaviour based on the EOS) was generated after recombination of the sample at reservoir conditions and used as a generic basis of the PVT behavior for the entire pad. It should be noted that a large concentration of H2S is coming from this type of oil and above 10%. The entire table set of the Vx Fluids IDs associated with the oil, water and gas properties are not presented in this document. But it should be known that they are automatically downloaded to the multiphase flow meter and represent the conversion of the different parameters from line to standard conditions and vice versa. Specific care was taken to account not only for water in liquid form, but also in vapor form.

5 OVERALL RESULTS

5.1 Dynamic Response Stage #1

During the Stage#1 of the Vx field trial, the meter was operated in “blind mode”, meaning that three phase flow measurements were successfully delivered in real time prior to the knowledge of the flowrate reference (i.e. separator test). Then, post-processing of the data was performed to report 4 phase flow measurements: Oil, water, natural gas and vapor flow rates. This was not implemented yet in the software version.

The figure 12 demonstrates the dynamic response to the flow of the Vx compared to the separator. The separator operating pressure is indicated in green, the Vx line pressure in blue, and line temperature in red. The high accuracy or performance is achieved via an optimal design of the inline venturi with a blind “T” for flow conditioning and then eliminating the issue due to change in flow conditions upstream of the meter. Moreover, this conditioning process allows getting faster thermo equilibrium at any conditions. The separator’s large vessel dampens the flow profile because of the need to keep the backpressure constant. The

pressure profile reveals that the separator pressure profile is flat while in reality there is a pressure fluctuation during the test.

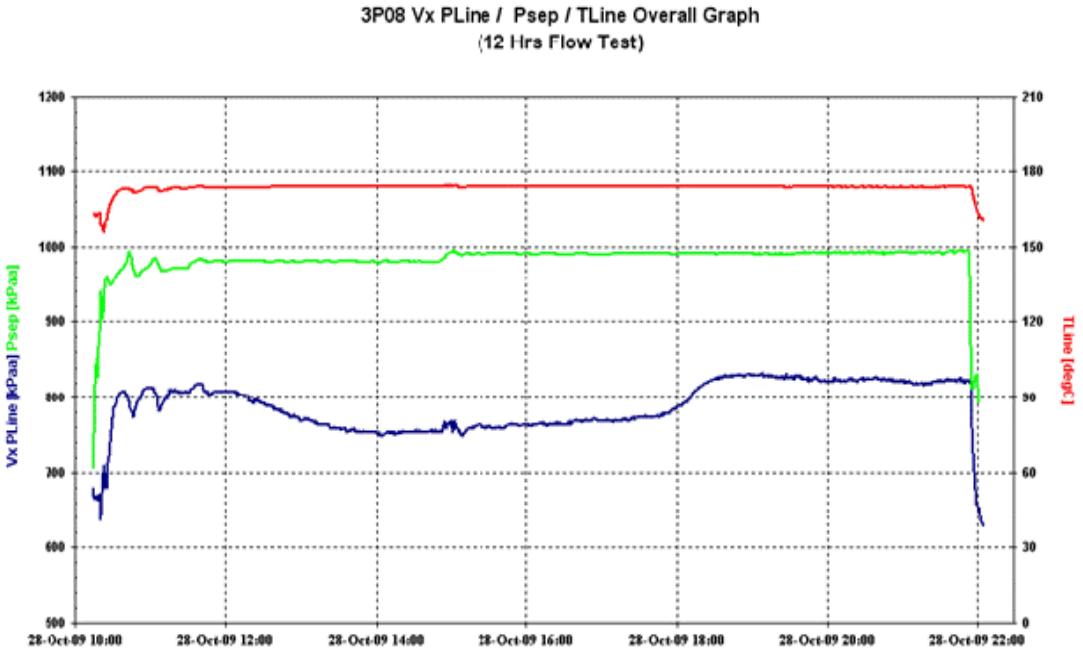

Figure 12: Field Operation and Equipment Proposed

The red line above confirms that wells were tested at an average of 180 °C flowing temperature or above. This demonstrates the capability of the Vx to operate at SAGD conditions.
The figure 13 shows a typical well recording versus time. A comparison Separator water cut, and Vx WLR is shown.

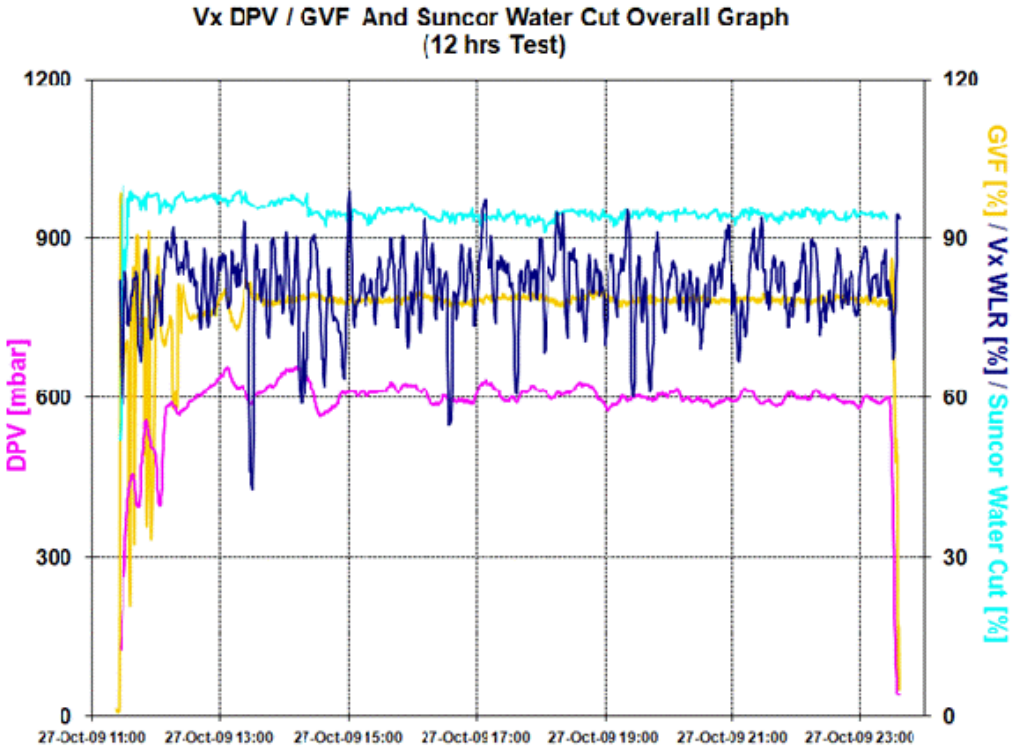

Figure 13: Field Operation and Equipment Proposed

The results from the Vx measurements indicate that the flow is turbulent and the WLR is never constant and always fluctuating. This could explain some of the large discrepancy between the reference water cut and the liquid sampling procedure (used as conventional system today inside SUNCOR) if unfortunately both comparisons are not synchronized. This aspect of the flow dynamic is important since it could affect the validity range of the test data and, therefore, the duration of each test.

The table 1 & 2 below present an overall performance summary for Stage 1 for all nine tested wells combined.

Table 1 – Measurement from Separator and Vx meter

Qmass Sep [kg/s]	Qliquid Sep [m3/h]	Density Liquid Sep [kg/m3]	CWE Sep Cor [m3/h]	WLR sep [%]	WLR sep* [%]	Qmass Vx [kg/s]	Qliquid Vx [m3/h]	Density Liquid Vx [kg/m3]	WLR Vx [%]	CWE Vx [m3/h]	CWE Vx [m3/h]
88.2	353.6	896.4	12.8	88.8	77.2	89.6	355.8	905.7	79.5	10.7	10.7

Table 2 – Comparison Separator – Vx Meter

Vx - Sep	Δ Qmass [%]	Δ Qliquid [%]	Δ Density Liquid [%]	Δ CWE [m3/h]	Δ WLR* [%]	Steam injected [kg/s]
12Hr	1.59	0.62	1.04	-0.04	**2.0**	196.3

*Corrected Values by using the proration factor for the entire field having no access to a proration factor ratio of the pad

The comparison between the Vx and separator WLR measurements shows a larger discrepancy on average for all the wells using raw data from the reference water cut meter. Vx reports consistently lower WLR values than the test separator in the blind test mode. Further examination revealed that the pro-ratio factors of the entire field were indicating an over-production of water and under-production of oil, i.e. the water cut at the separator was too high. In conclusion, there is a significant error with the current water cut meter installed and the technology proposed. The only way to try to do reconciliation is to correct based on the proration factor which was done and presented in the table 1 & 2.

It should be noted that in parallel 50% of the liquid samples collected have been analyzed in laboratory, and compared with the Vx measurements. They are well within the specification with in average 1% absolute error based on the analysis of few wells. It should be noted that with the same wells, there is large a discrepancy between the manual sampling done at the separator and the WLR read from the water cut meter, and then confirmation the correction applied above.

To summarize the main results from Stage#1:

- Continuous flow measurements provided for each well revealed good dynamic response
- Benchmarked resulted between the Vx meter and the test separator equipment are similar
- Total liquid mass flow rates are better than 2%
- Liquid densities are within 1%
- Recalculated WLR within 2%
- WLR within 1% versus half of the samples analyzed to demonstrate the WLR validation form the Vx.
- No safety or reliability issues during Vx meter testing

5.2 Measurement Reproducibility Stage #2

To demonstrate the reproducibility of the flow measurements using the Vx technology, a second test was completed, and this time shortening the flow period from 12 hours to 6 hours. It is important to mention that only, Well A, B and C were the wells that preserved the same flowing conditions (frequency, tubing choke size, tubing, and casing steam injection rate) during both tests. This set of data is highlighted inside the Table 3.

Due to the fluctuation of the initial conditions it was then proposed to playback, the data initially recorded over 12 hours but only during the 4 first hours. This will then show the stability of the measurement and then the capability to establish the performance of a well on a shorter period. It can be also interesting to note that the recorded raw data can always be playback at any time. This could be instrumental for SUNCOR to demonstrate to ERCB the performance of the well or be able to recompute data if a wrong setting was done on a multiphase Vx meter, this is a unique feature of the technology.

With the Vx meter only, the data of the 12 hours testing were reprocessed for only 4 hours showing a good agreement with the original 12 hours test. This supports the idea that the well tests, if only done periodically, can be significantly shortened from the current separator-based operation.

Table 3 – Overall performance with 12, 8 and 4 hours recording

Well	Tubing Choke Size %			Frequency Hz			Tubing Steam Rate m3/hr			Casing Steam Rate m3/hr			GVF %		
	12hr	6hr	4hr	12hr	6hr	4hr	12hr	6hr	4hr	12hr	6hr	4hr	12hr	6hr	4hr
A	45	45	45	39	39	39	4.0	4.0	4.0	10.0	10.0	10	95	96	96
B	55	55	55	41	41	41	4.0	4.1	4.0	8.0	8.0	8.0	97	97	97
C	100	100	100	0	0	0	6.0	6.0	6.0	34.0	34.0	34.0	98	98	98
D	45	100	45	56	54	56	4.0	5.0	4.0	35.0	16.0	35.0	78	80	78
E	35	40	35	53	50	53	8.0	4.0	8.0	35.3	8.0	34.0	62	68	62
F	45	40	45	55	55	55	8.0	4.0	8.0	25.0	8.0	25.0	21	56	23
G	52	50	52	54	52	54	8.0	4.0	8.0	21.9	7.9	22.2	50	49	48
H	40	40	40	49	49	49	8.0	4.0	8.0	20.0	7.9	19.9	79	77	79
I	65	65	65	57	55	57	4.0	4.0	4.0	7.9	10.9	8.0	78	79	78

Only the wells highlighted in gray kept exactly the same operating conditions during both tests.

As an example, well production measurements for one well is plotted (see Figure 14, 15, and 16) for the 12 hours, 6 hours, and 4 hours tests. The line temperature is presented in red, line pressure in blue, liquid flow rate in yellow and gas flow rate in light blue.

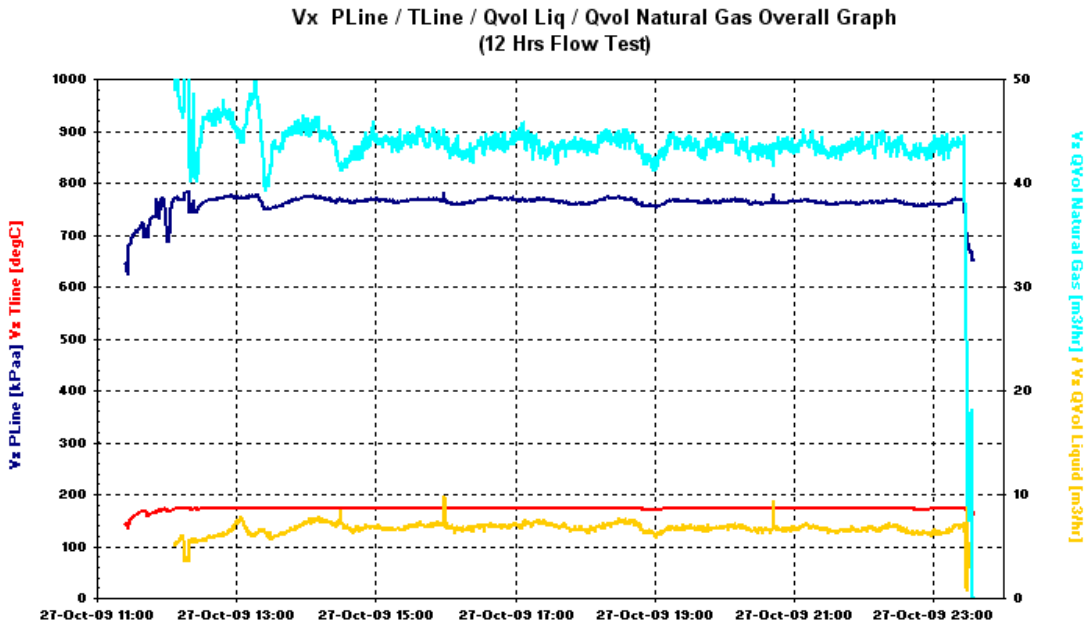

Figure 14: Pressure, Temperature, Gas & Liquid flow rate over 12 hours

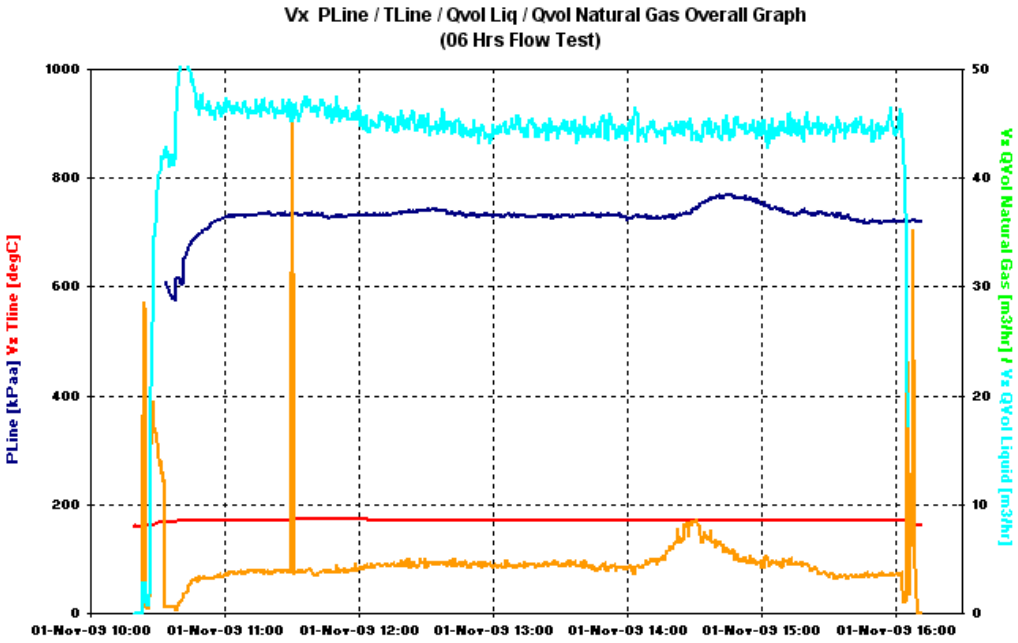

Figure 15: Pressure, Temperature, Gas & Liquid flow rate over 6 hours

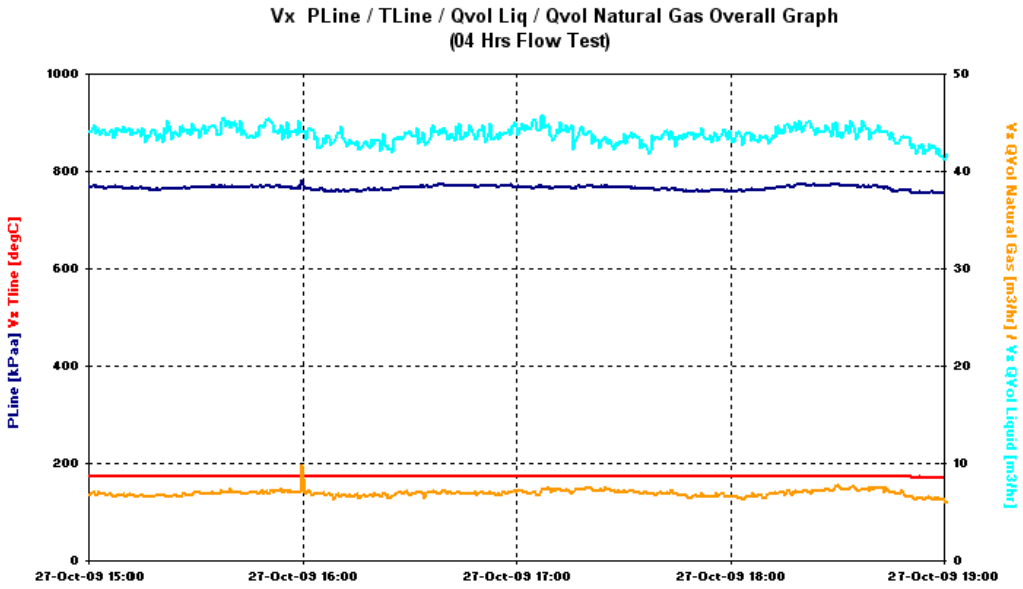

Figure 16: Pressure, Temperature, Gas & Liquid flow rate over 4 hours

Table 4 presents a comparison summary on a well-by-well basis for the 12-hour, 6-hour, and 4-hour tests.

Table 4 - The Table Pressure, Temperature, and Condensed Water Equivalent for 12, 8 and 4 hours

Well	Vx Pline (kPaa)			Vx Tline (DegC)			CWE (m3/h)		
	12hr	6hr	4hr	12hr	6hr	4hr	12hr	6hr	4hr
A	656.4	661.6	647.9	167.4	167.6	167.8	1.21	1.30	1.23
B	804.9	799.1	813.0	178.2	178.2	178.2	2.56	2.56	2.59
C	855.7	851.6	850.4	183.1	183.0	183.2	3.75	3.71	3.75
D	838.2	772.5	838.4	176.6	174.5	176.6	0.80	0.77	0.79
E	857.2	771.9	857.5	175.6	172.8	175.5	0.39	0.47	0.40
F	766.3	667.4	767.0	168.2	164.9	168.2	0.40	0.18	0.40
G	788.7	685.9	762.9	174.1	166.6	174.2	0.26	0.18	0.24
H	764.8	736.8	765.6	172.2	171.7	172.2	0.66	0.59	0.66
I	757.6	736.4	757.6	172.3	171.5	172.3	0.66	0.64	0.67

Table 5 – Liquid Mass Flow rate, WLR comparison for 12, 6 and 4 hours

Well	Liquid Mass (kg/s)			WLR		
	12hr	6hr	4hr	12hr	6hr	4hr
A	4.1	3.8	4.0	59.4	44.3	59
B	5.3	5.2	5.2	77.4	71.8	71.8
C	5.4	5.4	5.4	80.7	77.3	81.7
D	12.8	11.8	13	84.2	79.7	83.5
E	13.6	13.2	13.5	84.3	82.9	81.4
F	9.7	10.0	9.6	85.7	84.6	85.1
G	16.3	13.2	16.3	79.7	82.4	79.6
H	11.0	11.2	11	80.6	81.3	81.3
I	11.4	10.9	11	83.9	78.6	83.5

WLR measurement performance decreases with a GVF increasing, when the GVF average over 10 seconds is above 96-98%, a cut off value has been applied in this case (i.e. No calculation of WLR measurement if the value is above of the cut-off) in order to reduce the noise associated with the measurement. It should be noted that a sluggy behavior will be more favorable and will guarantee a better performance even if in average the GVF was above 96-99%.

The presented data above confirms that the measurement are identical for a 12 hours test versus the 6 hour test and even so the conditions may not have been entirely identical there is a good repeatability over 4 hours test. These results reveal that testing for shorter period of time and more frequently is providing the same level of confidence in the measurement, and then it is possible to do more frequent tests and then get a better performance of the production of each well over time.

5.3 Gas/Oil Ratio Reporting

The natural gas and vapor inside the flow stream could be obtained with an equation of state developed specifically for SAGD operation for SUNCOR. IA summary of the results for the vapor phase and SOR results (average of the 12hrs test) is shown below.

Table 6 – Total Gas, Natural Gas and GOR measurements

Well	Total Gas Flowrate [Sm3/h]	Natural Gas Flowrate [Sm3/h]	GOR [Sm3/Sm3]
A	1496.0	39.4	7.3
B	3428.8	15.0	1.6
C	5118.2	26.6	2.5
D	1111.4	1.3	0.3
E	587.4	14.9	1.8
F	93.43	2.1	0.9
G	441.4	2.92	0.2
H	912.7	6.9	1.1
I	900.4	6.5	1.2

5.4 Sampling Verification

The table below presents a comparison of WLR measurements from Vx, Separator, Vx Sample, and Manual Samples for each of the four sampled wells.

Table 7 – Comparison Vx measurement, sampling at the Vx, Separator Measurement and sampling at the separator

Well	Vx Sample	Vx Real-Time	Separator Real-time	Manual Sampling	GVF
A	85	69	93	56	96
B	73	77	80	72	98
C	77	80	79	72	80
D	74	79	80	80	81

It is important to mention that well B was a natural lifted well and this is the primary reason of an average GVF around 98%. This well was also very challenging to test. The Vx real-time measurement reported in this table was calculated over the same 15 minutes period of time when the Vx and Separator samples were taken except for the cases above 96%.
For the wells with a GVF below 96%, the results show a good match of the Vx real time WLR measurements with the reference samples.

5.5 Test Conditions

One of the important reliability considerations was to ensure that the Vx flow meter could operate at the extreme cold conditions during the winter season without any performance issues. During the second month of the Vx trial at Firebag ambient temperatures close to -40C were happening. The figure 32 shows a thermometer recording an ambient temperature (without wind chill factor) of -37.1 C at the well site.

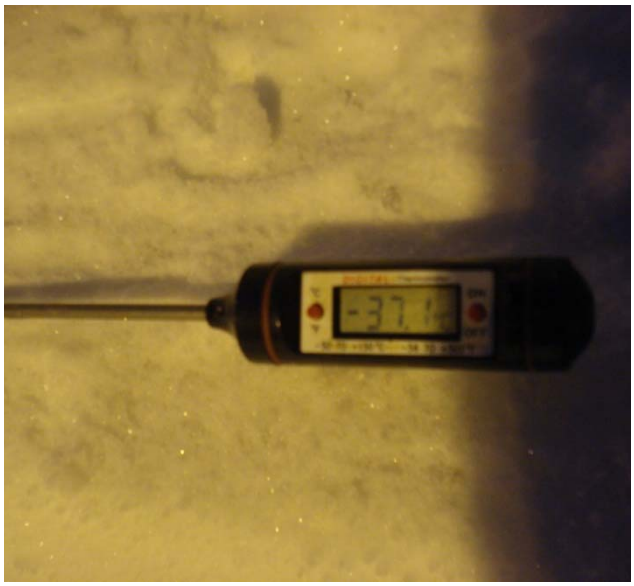

Figure 17: Field conditions in Canada in December

The meter itself has been used most of the time with or without hot air supply and working in the range of -15 to +15 DegC without showing any change in the performance. Data Recording beyond -20 DegC (ambient temperature at the meter) has been also done in exceptional cases and have demonstrated the robustness of the Vx technology in winter conditions, the issue being if working to too low temperature being to plug the small liner very quickly.

The Figure 18 shows additional views of the test conditions at Suncor Firebag. The truck was equipped with a logging cabine and was self autonomous (electricity, warning system).

Figure 18: Field Operation Deployment

It will be recommended to leave the meter like in other cold country either in container (Alaska or Kazakhstan Design). Due to the high temperature of the flow, the ambient temperature inside the box will be kept at least in the range of -15 degC to 15 degC in the worst case and then this will not need any additional heating as demonstrated in the qualification test.

4.6 Summary

As demonstrated during this trial, the Vx technology provided better accuracy compared to the test separator data and allowed for more frequent well testing and then better well performance monitoring. The flow dynamics could be better monitored and understood in real time with fast acquisition measurements instead of the conventional test separator methods. An overall summary of the performance of the Vx meter versus the separator and the short duration test is shown below in the table below. This represents the average of the entire pad (9 of the 11 wells):

Table 8 – Overall production of the 9 wells for separator and Vx with 12 and 6 hours recording

Sep & Vx	Qmass Sep [kg/s]	Qliquid Sep [m3/h]	Density Liquid Sep [kg/m3]	CWE Sep Cor [m3/h]	WLR sep* [%]	Qmass Vx [kg/s]	Qliquid Vx [m3/h]	Density Liquid Vx [kg/m3]	WLR Vx [%]	CWE Vx [m3/h]	CWE Vx [m3/h]
12Hr	88.2	353.6	896.4	12.8	88.8	89.6	355.8	905.7	79.5	10.7	88.2
6Hr	82.6	331.8	898.1	12.9	86.4	85.3	337.9	907.9	75.9	10.4	82.6

Table 9 – Overall comparison of the 9 wells for separator and Vx with 12 and 6 hours recording

Vx - Sep	Δ Qmass [%]	Δ Qliquid [%]	Δ Density Liquid [%]	Δ CWE [m3/h]	Δ WLR [%]	Steam injected [kg/s]
12Hr	1.59	0.62	1.04	-0.04	2.0	196.3
6Hr	3.27	1.84	1.08	-0.05	-1.3	113.3

Table 10 - Overall production of the 9 wells for Vx with 12 and 4 hours recording

Vx12 Vx4	Qmass Vx12 [kg/s]	Qliquid Vx12 [m3/h]	Density Liquid Vx [kg/m3]	CWE Vx12 [m3/h]	WLR Vx12 [%]	Qmass Vx4 [kg/s]	Qliquid Vx4 [m3/h]	Density Liquid Vx4 [kg/m3]	CWE Vx4 [m3/h]	WLR Vx4 [%]
Total	89.3	355.7	905.7	10.7	79.5	89.5	353.9	912.6	10.7	78.5

Table 11 - Overall comparison of the 9 wells for separator and Vx with 12 and 6 hours recording

Vx12 Vx4	Δ Qmass [%]	Δ Qliquid [%]	Δ Density Liquid [%]	Δ CWE [m3/h]	Δ WLR [%]	Qgas [m3/h]	D Qgas [m3/h]	GVF [%]
	-0.11	-0.51	0.76	0.04	-1	284.7	2.8	76.5

There are comparable results measured by Vx meter and by test separator equipment:

- Total liquid mass flow rates are better than 2%
- Liquid densities are within 1%
- WLR Vx versus WLR separator recalculated is within 2%

6 OPTIMIZATION

SAGD well production is composed of and controlled by many man-made variables that are not found in conventional production operations. These range from initial steam injection – for steam chamber creation and oil heating, to ramp up – with gas lift injection, steam lift, gas lift, electro-submersible pumps (ESP) / progressive cavity pumps (PCP) lift, to blow down and also to break through.

In artificial lift systems, a variety or mechanical and systemic components can limit optimization of system usage. For example, artificial lift components may be blocked, damaged, sized improperly, or operated at less-than-optimal rates.
Maintaining the ESPs within a good envelope of operation is critical to optimization. A real-time optimization SAGD framework could be used to detect certain specific mechanical or systemic problems at the pump, identify the cause of underperformance, and take preventive measures that can increase the ESP run-life and decrease production downtimes.
ESPs are working in a harsh environment and it is advisable to reduce as much as possible the mechanical stress and/or large flow rate variations. ESP performance is altered by frequency changes due to changing production conditions; it is important to try to work in the best operating range, which leads to have the proper sizing. Optimization is also linked to efficiency, which is not only performance, but also efficient use of power.

With Vx technology, it is possible to perform real-time production optimization by adjusting the frequency control of the pump based on the Vx response. The Vx technology can deliver real-time production information since no stabilization of flow periods is required. The Vx is also not dependant on flow regimes and its high-speed acquisition frequency provide results even when the well production is unstable, giving the full picture of the flow dynamics when the frequency of the ESP is changed for optimization purposes.

When available, real-time flow measurements obtained from the Vx can be applied against a reservoir simulation/well model. Discrepancies between the measured data and the model can be used to determine factors contributing to sub-optimal SAGD performance and make decisions in a timely manner.

The protocol for Stage #3 was to test the West side of Pad. The pump running frequencies was to adjust from the initial operating frequency in 2 Hz intervals or so every three hours in order to capture a representative range of performance of the pump and well system.

The main objective of this stage of the test was to investigate the response of the Vx measurements to changes in the pump frequencies steam injection rates and chokes. If real-time measurements can be obtained, this opens the door for a future implementation of a SAGD optimization method that can result in increased productivity, less energy consumption and increased ESP run life.

Five wells were selected for the optimization trial, this stage of the trial consisted of a 12 hours baseline test at a fixed frequency and tubing pressure set point followed by another 12-hour test with a frequency change every four hours. A minimum of three frequency changes were made per well. Each frequency change was only made after the well had stabilized, and only if there was room on the pump curve to make the next frequency change. We show you a typical raw data curve.

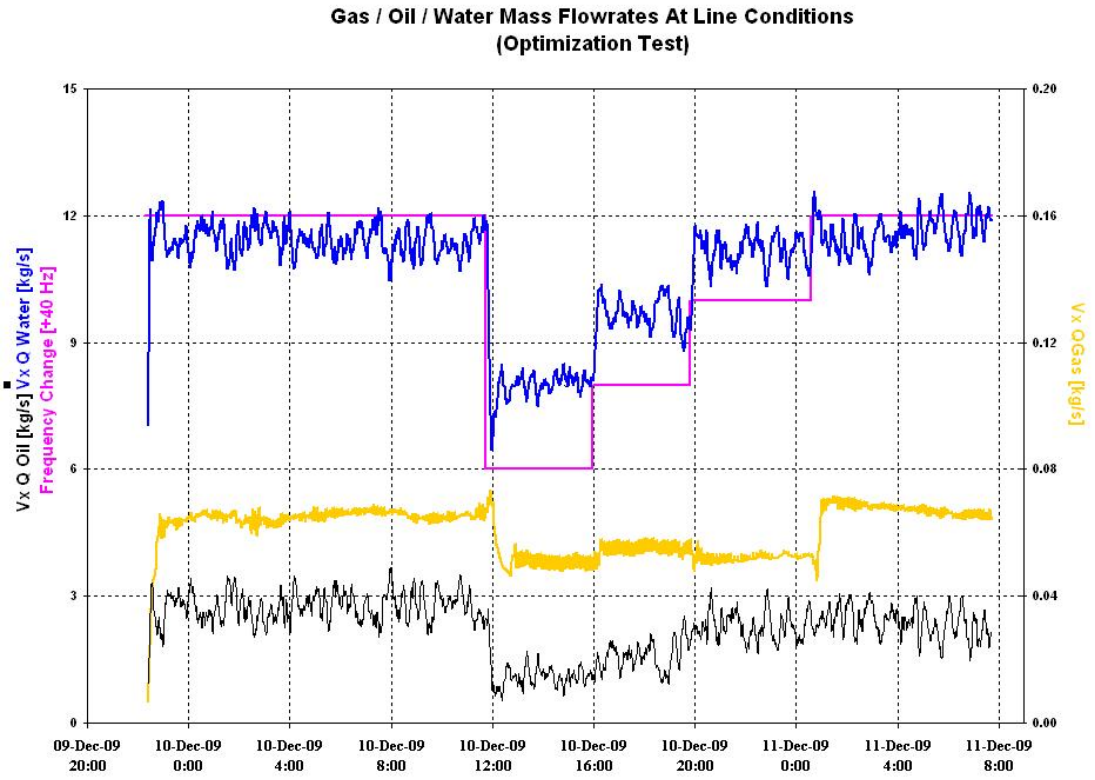

Figure 19: Concept of optimization of each well (data recorded vs. Time)

7 SUMMARY

This paper presents the results of an extensive evaluation on the use of Multiphase Flowmeters (MPFM) based on the Vx Technology to monitor production flow rates in SAGD wells at the Suncor Firebag Project.

The collaboration between Schlumberger and SUNCOR to test and qualify the multiphase technology started in 2007, when a single-well field trial was carried out at the Firebag project facilities. This was the first introduction of the technology to SAGD environments. In 2009, a second and more advanced field trial was initiated. A pad was selected due to the large number of good producing wells and ideal set up of the conventional equipment.
9 wells from Pad 103 were tested during the months of October and December 2009, ensuring that the MPFM was challenged against the full range of operating conditions of the SAGD wells. During two months of extensive well testing and fluid sampling, no safety incidents were encountered and the MPFM reported well production rates continuously and without any performance degradation even during the extreme ambient temperatures recorded at the well site.
Flow measurements between the MPFM and the Test Separator for the same stable flow periods revealed consistent results between both equipments. Total liquid mass flow rates are within +/- 2% and liquid densities within +/- 1% on average.
The comparison between the Vx and separator Water-Liquid Ratio (WLR) measurements showed a discrepancy for all the wells comparing the raw data. The Vx reports consistently lower WLR values than the test separator. Further examination revealed that the pro-ratio factors were indicating a fair over-production of water and under-production of oil for the entire field, i.e. the water cut at the separator was too high. In conclusion, there is a significant error with the current water-cut meter at the opposite of the Vx Technology.

In order to obtain a more accurate reference for comparison, the information about the pro-ratio factor for the entire field was used to back-calculate what should have been the WLR separator-based measurement, resulting in WLR Vx versus the recalculated WLR (from separator) to be within 2%.If the Vx had been used in this field during the test period (using the data from the Vx) one would have obtained a proration factor (for this pad) between 1.02 and 0.98 for oil and water over the two months (production sold versus what was reported by Vx).
To demonstrate the reproducibility of the flow measurements using the Vx technology, a second stage was completed, this time shortening the flow period from 12 hours to 6 hours. Then, with the Vx meter only, the data of the 12 hours testing were reprocessed for 4 hours showing a very good consistency in the results with the 12 hours test.The main conclusions of the test are as follows:

8 CONCLUSIONS

The main conclusions of the test are first that all the initial objectives given for the testing program were met or exceeded. Second, the Vx multiphase meter managed to demonstrate all the operating requirements required by Suncor operations. The uncertainties of all the phases are as per below:

- Uncertainty of within +/- 2% (after correction of the reference measurement based on a global back allocation factor)
- Uncertainty of minimum +/- 2% on Liquid rate
- Uncertainty of +/- 2% on Total Gas Flowrate (due to wet gas conditions and assuming that it is only steam)

Third, the Vx technology was capable to capture the entire dynamic of the flow: Start-up, intermittent and pulsing flow. The meter was used above 180oC in this test. By the order of accuracy form the output of the meter, the sequence is as follows: Total mass (or volumetric) flow rate, liquid mass (or volumetric) flow rate, gas mass (or volumetric) flow rate, GVF, GLR, then WLR, and associated oil and water flow rate.

The Vx meter reveals good dynamic response, repeatability and accuracies of the flow rates and has shown promise to be able to be used as an optimization tool. This is likely the result of the design and robustness of the Vx meter, summarized with some key features such as no Tuning Factor, no Separation, no Flow Calibration, no issues with Foams or Emulsions, no moving part, no sensors in direct contact with the fluid, and improve water detection and accurate BSW monitoring.

4 REFERENCES

[1] Performance of Combination of a Venturi and Nuclear Fraction Meter in SAGD Production Operations. Hompoth, Daniel, et al. Edmonton : s.n., 2008. World Heavy Oil Congress. 2008-422

[2] Multiphase Metering: Importance of Fluid Property Knowledge in SAGD Operations. Hompoth, Daniel, Pinguet, Dr. Bruno and Guerra, Elsie. Edmonton : s.n., 2008. World Heavy Oil Congress. 2008-421

[3] SAGD Production Optimization: Combination of ESP and Multiphase Metering Bruno G. Pinguet, Elsie Guerra and Colin Drever,Schlumberger. Edmonton : s.n., 2008. World Heavy Oil Congress. 2008-424

[4] Conventional metering issues for thermal in situ production of extra heavy oils and improvement of a commercial nucleonic multiphase meter for such applications. V. Arendo F. Dang and B. Pinguet, PH. Pechard, JL. Roudil. Margarita Island : World Heavy Oil Congress, 2009. 2009-327

North Sea FLOW Measurement Workshop

Paper 7.2

Multiphase Flow in Coriolis Mass Flow Meters – Error Sources and Best Practices

Joel Weinstein
Emerson Process Management – Micro Motion, Inc.

TÜV SÜD

nel technology for life

28th International North Sea Flow Measurement Workshop
26th – 29th October 2010

Multiphase Flow in Coriolis Mass Flow Meters – Error Sources and Best Practices

Joel Weinstein, Emerson Process Management – Micro Motion, Inc.

1 INTRODUCTION

Coriolis mass flow meters are used throughout the oil and gas industry, from upstream allocation and net oil measurement to custody transfer of pipeline quality oil. Coriolis meters have an inherent advantage over volumetric meters in measuring pure liquid quantities in applications involving liquids with entrained gas because the mass flow rate of an aerated mixture is close to that of the liquid flow rate. Likewise, volumetric meters may be preferred for measurement of wet gas, as the volumetric flow rate of a wet gas is close to that of the gas flow rate, which is typically the desired quantity. With that in mind, multiphase flow in the context of this paper refers to any mixture of two or more components in which the base phase is a liquid. This includes bubbly liquids, particle-laden flows, slurries, emulsions, and multi-liquid mixtures.

Coriolis meters are unique in using two oscillating flow tubes to make measurements, with the assumption that the fluid moves directly with the tubes in the oscillatory direction. When multiple phases or components of different density are present, this assumption is not valid and errors result. Measurement accuracy is reduced due to various effects, and the extent of the error is a complicated function of meter design parameters, fluid properties, and flow conditions. Recent research conducted by Coriolis meter manufacturers has led to significant improvements in performance in multiphase applications. For example, modern signal processing algorithms allow resolution of flow signals even in the presence of increased flow noise. However, some multiphase errors remain. Understanding the true physical mechanisms for these remaining errors allows for development of an effective set of installation and operational best practices for multiphase applications. It will be shown that these practices can substantially reduce measurement error and make Coriolis meters a legitimate solution in multiphase applications involving relatively small gas or particle volume fractions.

The paper includes a clear explanation of the dominant error mechanism in multiphase Coriolis measurement, termed *decoupling*, which occurs when gas bubbles or solid particles move relative to the surrounding liquid during vibration of the flow tube. A theoretical analysis of decoupling, along with real-world test results, highlight the importance of several parameters including base phase viscosity, second phase particle size, vibration frequency, and density ratio between the phases. Many of these parameters, such as particle size, are directly influenced by installation and operation practices. Recommendations are made for simple practices which allow users to optimize measurement performance in the presence of entrained gas or solid particles. Several specific oil and gas applications are discussed – live oil with entrained gas, net oil, watercut, cementing, and fracture sand applications.

The paper concludes with a discussion of an important real-time diagnostic for detection of multiple phases, which is applicable to any Coriolis meter in any multiphase scenario, including water and oil measurement and solid-laden flows. Historically, density has been used for detection purposes; however, density is influenced by changes in temperature, pressure, and composition, and is not particularly sensitive to low levels of entrained gas or solid particles. Early and accurate detection of the presence of multiple phases with a Coriolis meter is best accomplished by monitoring the amount of power consumed during flow tube vibration. The same physical mechanism which causes errors in multiphase measurement, decoupling, also dramatically increases power consumption due to the relative motion between gas or solid particles and the surrounding liquid. With the use of this diagnostic, the Coriolis meter can provide an extremely sensitive detection of multiple phases. This is particularly useful in oil and gas applications in which multiphase flow is not expected and is rather a cause for alarm, for example custody transfer of pipeline quality oil or allocation measurement downstream of a separator.

1.1 How to Read this Paper

This paper is written for a diverse audience, and is accessible to anyone with a basic technical background. It is not necessary to get lost in the details of the equations in Section 3 to understand the most important information regarding how to use Coriolis meters in multiphase applications. If time is short or you're looking for an overview, please consider skimming Sections 2.3, 3.1, and 3.2, and rejoin at Section 3.3. Experienced users of Coriolis meters may want to skim Section 2.1 and rejoin at Section 2.2. The most important part of the paper is Section 4, so if you're very short on time, read Section 2.2, then skip to Section 4.

2 CORIOLIS MEASUREMENT IN MULTIPHASE FLOW

Coriolis meters are potentially more accurate than volume-based devices when gas is present in the process fluid because gas adds very little mass but a large volume. Users almost always require pure liquid or gas quantities, not mixture quantities. When 10% gas volume fraction is entrained in a flowing fluid, a volume-based device will measure about 10% high in liquid volume flow rate, while a Coriolis meter will measure nearly the correct liquid mass flow rate due to the negligible mass contribution of the gas. However, when multiple phases are present, some of the basic assumptions made in Coriolis measurement break down and errors may result. In order to study the failure modes, it is first useful to briefly review how the density and mass flow measurements are made.

2.1 Coriolis Measurement Basics

The Coriolis meter measures mass flow and density of single phase gas or liquid flows to very high accuracies. There are no complex moving parts that wear out over time and minimal installation requirements. Because mass is always conserved, pressure and temperature measurements are unnecessary and equations of state are not needed when measuring mass flow. The Coriolis meter is therefore practical in applications involving chemical reactions, which are based on a mass balance, as well as applications involving a compressible fluid or in which temperature and pressure vary significantly. However, due to their unique design, Coriolis meters do have some inherent design challenges. For example, temperature and pressure variations affect the vibrating tube by causing modulus changes and material expansion. These and other effects are usually compensated out.

A common Coriolis meter design consists of two flow tubes oscillating 180° out of phase at the natural frequency. The vibration of the tubes about fixed points yields a rotating, non-inertial reference frame in which forces such as the Coriolis force are present. As shown in Figure 1, the flow separates into two tubes after entering the meter. The tubes are driven by a magnet and coil assembly at the first bend mode resonant frequency with a periodic signal at the location marked driver. The oscillation frequency depends on the mass and stiffness of the system. If the fluid in the tubes is very dense, the tubes will be heavier, resulting in a decreased natural frequency. For a low density fluid such as a gas, the frequency will be higher. After calibration on a high and low density fluid, the density of an unknown fluid can be determined by measuring the frequency of oscillation of the tubes. The actual measurement is made using two additional magnet and coil assemblies, called pickoffs, mounted between the tubes at measurement

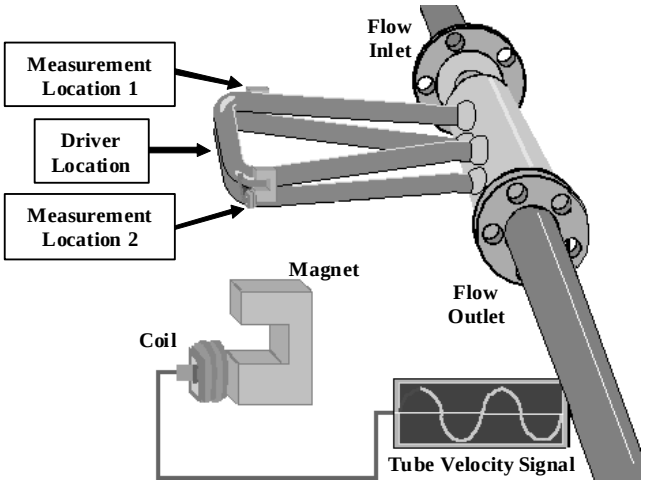

Fig. 1 - Anatomy of a Coriolis flow meter

locations shown in Figure 1. The pickoffs create a relative velocity signal which can be processed to find the oscillation frequency.

Fluid particles travelling through the oscillating flow tubes experience a Coriolis force due to the rotating reference frame. At any instant, this force applies in the opposite direction on the inlet and outlet side of the meter (see Figure 2), exciting a twist motion which is superimposed on the normal bend motion (see Figure 3). Here, a fluid parcel of mass *m* moves at velocity *V* in a flow tube with angular frequency *ω*, resulting in an applied Coriolis force, F_c, on the flow tube by the fluid. The twist motion results in a time delay, ΔT, between the inlet and outlet side of each tube which is measured using the signals from the two pickoffs.

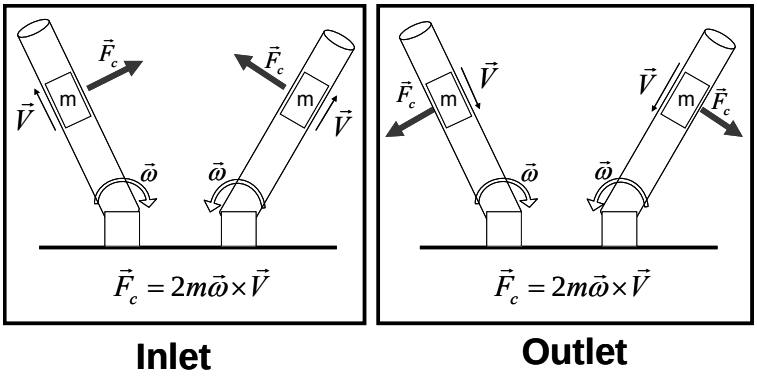

The magnitude of the time delay is linearly related to the mass flow rate through the meter because the Coriolis force increases linearly with the product of mass and velocity. After calibration, the Coriolis meter can measure an unknown mass flow rate using the time delay between the inlet and outlet sides of the tubes.

Fig. 2 - Coriolis forces on the inlet and outlet flow tubes

2.2 Decoupling Effects

A pure liquid moves in the transverse direction exactly with the flow tubes, and the center of gravity of the fluid remains fixed in the middle of the tube. However, the presence of two phases with different density causes a decoupling of the transverse fluid motion from the tube motion. For example, liquid particles and gas bubbles of the same volume will be accelerated differently due to the difference in their mass. Gas bubbles experience higher acceleration than the surrounding fluid which leads to relative motion between the bubbles and the fluid. This causes mass and density measurement errors due to changes in the location of the center of gravity of the fluid mixture inside the tube.

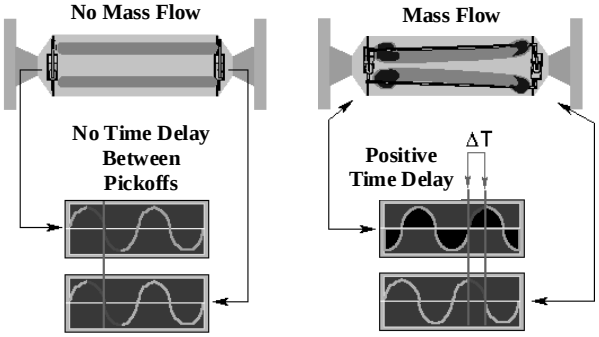

Fig. 3 - Top view of tubes showing twist mode

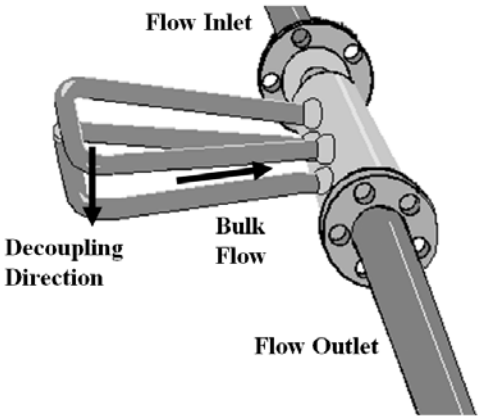

Fig. 4 - Direction of decoupling and bulk flow

The term "decoupling" refers to relative motion between two components of differing density in the direction of tube oscillation, which is perpendicular to the direction of bulk fluid flow, as shown in Figure 4. To model decoupling, it is not necessary to know exactly how the particles move through the meter, which would be very difficult due to the multiple phases and complex geometry of the flow tubes. Instead, the critical quantities are found to be the amplitude ratio and phase delay between the particle and fluid in the transverse direction.

Figure 5 shows a cross-sectional view of a single vibrating tube at two instances during a vibration cycle. At the point of maximum deflection, the bubble has moved further than the fluid by a factor defined as the decoupling ratio, A_p/A_f. The amplitudes are defined with respect to the distance from the midpoint of tube oscillation.

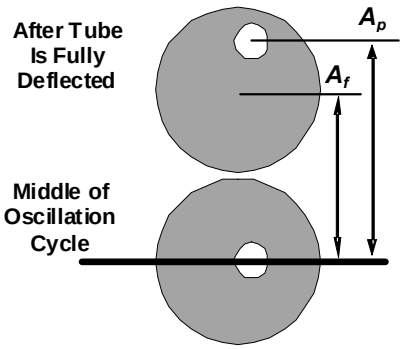

Fig. 5 - Decoupling ratio definition

Decoupling causes some of the liquid mass in the tubes to move so that it is undetected by the flow meter. This causes the density to read lower than the mixture density in the case of a bubbly fluid. For example, if a mixture consists of 10% volume fraction gas in a liquid of density 1000 kg/m^3, then the meter density should read 10% lower than the liquid, or 900 kg/m^3. However, due to decoupling, the meter erroneously measures perhaps 898 kg/m^3. The further the bubbles or particles decouple from the fluid on each oscillation of the tubes (ie. greater A_p/A_f), the larger the undetected volume of fluid will be and the larger the resulting error. Mass flow is also affected by decoupling, causing the meter to under-predict flow.

Figure 6 shows a schematic of the facility at Emerson Process Management - Micro Motion for testing entrained gas performance of Coriolis meters. Reference Coriolis meters are used for precise mass flow measurement of the separate liquid and gas streams. The reference mixture mass flow through the test meter is simply the sum of these two streams. Pressure (P) and temperature (T) measurements upstream and downstream of the test meter are used to calculate the volume fraction of the gas inside the meter, which gives mixture density. After flowing through the test meter, aerated fluid is returned to a tank and sufficient residence time is allowed for full separation of gas and liquid phases.

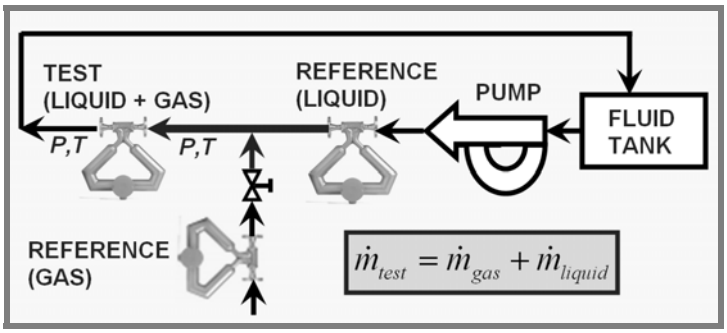

Fig. 6 - Multiphase test facility schematic

Figure 7 shows percentage mass flow error from true mixture mass flow in a Coriolis meter due to entrained gas. Pressure inside the meter is held constant at 210 kPa (30 psig) for all tests, while flow rate and the amount of gas injected are varied. For each test at constant mass flow rate, increased gas volume fraction results in increased measurement error. However, performance improves with increasing flow rate because the gas phase is broken down into very small bubbles rather than the larger slugs of gas which occur when pipeline velocities are low. This results in a more homogenous fluid mixture, and as will be shown later, smaller bubbles decouple from the fluid phase to a lesser extent.

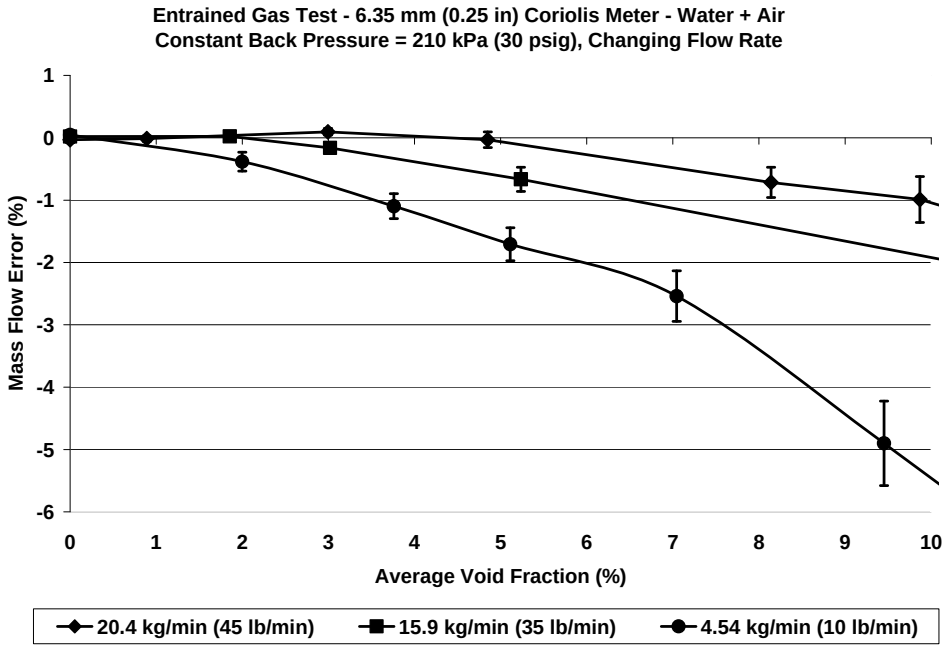

Fig. 7 - Mass flow error due to entrained gas

Density error from true mixture density is shown in Figure 8 for the same conditions. As expected, performance degrades with increasing void fraction and improves with increasing flow rate. Extensive experimental data has been obtained for a range of meters and fluids. For a definition of mixture density, see for example equation (18) in Section 4.2.

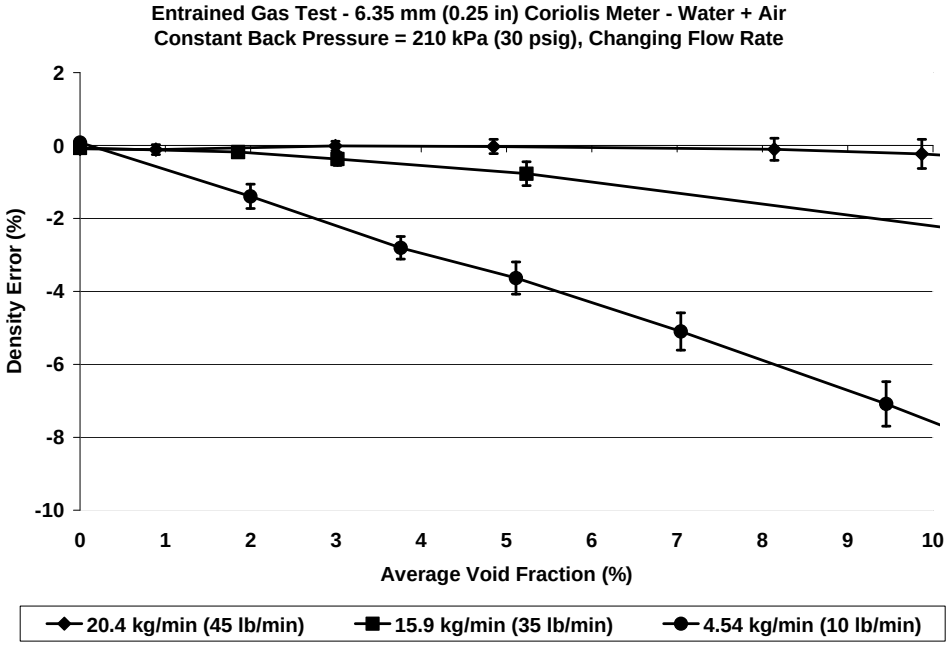

Fig. 8 - Density error due to entrained gas

In order to better understand the complicated sources of error in multiphase flow in a Coriolis meter, we constructed visualization meters out of clear polycarbonate tubing. Several sizes and shapes were made to investigate the differences between meter designs. In Figure 9, a 6.35 mm (0.25 in) dual curved tube meter is photographed with approximately 20% gas volume fraction in water with green food coloring. The flow rate is moderate in frame (a), but quite low in frame (b).

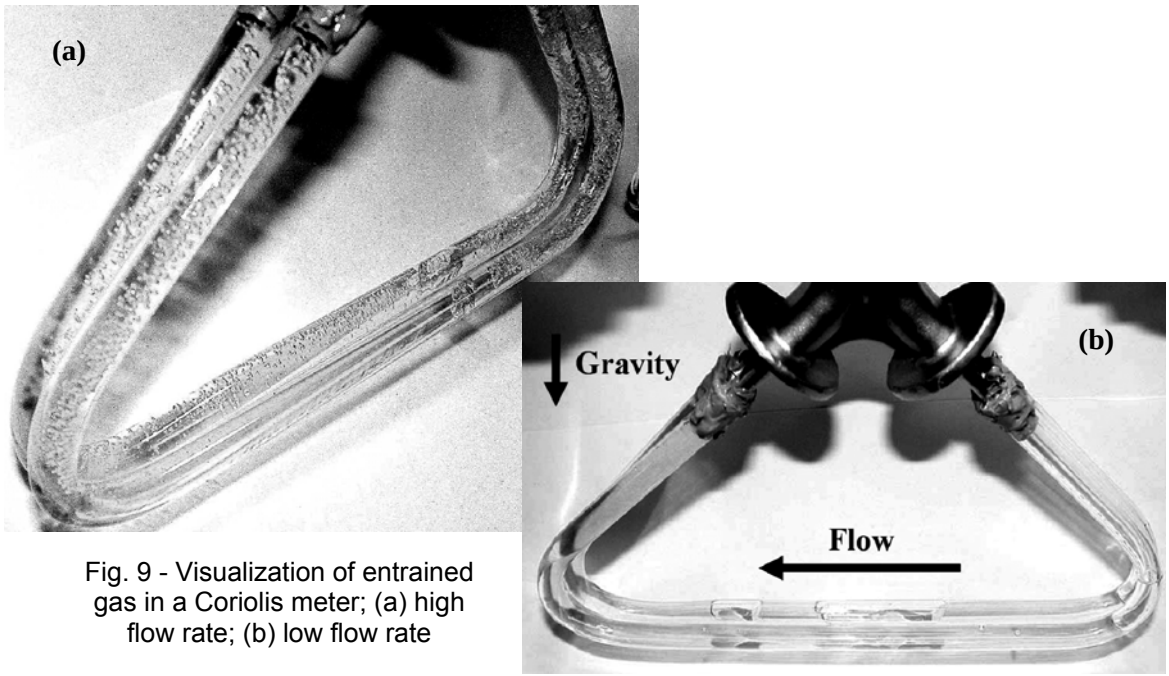

Fig. 9 - Visualization of entrained gas in a Coriolis meter; (a) high flow rate; (b) low flow rate

The bubbles are fairly well distributed within the flow tubes in frame (a) and the amount of gas in each tube is consistent. For this flow condition, errors would be small due to the homogeneity of the mixture and the small bubble sizes. However, at much lower flow rates, gas can accumulate on the inlet or outlet side of the meter depending on installation orientation and result in asymmetries along the length of the tube. Frame (b) of Figure 9 shows a scenario in which gas has accumulated on the inlet side due to positive buoyancy of the bubbles on the inlet side of the meter. Large slugs of gas are also seen near the middle of the tubes. The asymmetries in mass and damping caused by the trapped gas directly impact phase delay and cause large positive mass flow errors. If the bubbles accumulate instead on the outlet side of the meter, then the mass flow error is negative. In either case, following standard multiphase piping practices for minimum flow rates resolves these problems and results in a homogeneous mixture which is symmetric along the length of the tube.

2.3 Velocity of Sound Effects

In addition to problems caused by the relative motion of bubbles and particles, Coriolis meters experience velocity of sound effects when the sonic velocity of the measurement fluid is low or the oscillation frequency of the meter is high. Gases have lower sonic velocities than liquids, but the lowest velocities result from a mixture of the two. The addition of even a small amount of gas to a liquid results in a dramatic reduction in the velocity of sound of the mixture below that of either phase.

The oscillation of the flow tube produces sound waves that oscillate in the transverse direction at the drive frequency of the meter. When the velocity of sound of the fluid is high, as in a single phase fluid, the first acoustic mode for transverse sound waves across the circular conduit is at a much higher frequency than the drive frequency. However, when the velocity of sound drops due to the addition of gas to a liquid, the frequency of the acoustic mode also drops. When the frequency of the acoustic mode and the drive mode are close, meter errors result due to the off-resonance excitation of the acoustic mode by the drive mode. For low frequency meters and typical process pressures, velocity of sound effects are negligible with respect to the specified accuracy of the meter. However, for high frequency Coriolis meters, the velocity of sound can be low enough to cause significant measurement errors due to interaction between the drive and fluid vibration modes.

A more physical explanation of velocity of sound effects in Coriolis meters is that the fluid in the tube is compressed against the outside wall of the tube on each oscillation when the compressibility of the mixture is high enough to allow for such motion. In this way, velocity of sound effects are similar to decoupling effects in that the actual error is caused by movement of the location of the center of gravity. The difference is that velocity of sound effects result in heavier fluid pushed to the outside walls of the tube while decoupling results in heavier fluid pushed to the inside walls of the tube. For this reason, velocity of sound errors are positive and decoupling errors are negative. This is confirmed by a recent model by Hemp & Kutin [1], which quantifies density and mass flow errors due to velocity of sound effects. The closed form expressions are given as percentage increases from true mixture values, where d is the inner diameter of the Coriolis meter flow tube, ω is the angular oscillation frequency, and c_m is the mixture velocity of sound.

$$\rho_{vos,err} = \frac{1}{4}\left(\frac{\omega d}{2c_m}\right)^2 \times 100 \tag{1}$$

$$\dot{m}_{vos,err} = \frac{1}{2}\left(\frac{\omega d}{2c_m}\right)^2 \times 100 \tag{2}$$

The remainder of this paper will focus on decoupling errors, which by comparison are poorly understood and are usually of greater magnitude than velocity of sound effects. For example, consider a 100 Hz Coriolis meter with 10 mm diameter tubes measuring oil with 1% gas volume fraction at low pressure. Density can be in error by up to 2% due to decoupling, but equation (1) predicts only a 0.02% error from velocity of sound effects. Also, velocity of sound effects can be easily avoided by using low frequency meters for multiphase applications, while errors due to decoupling are more difficult to eliminate.

3 OSCILLATORY PARTICLE DYNAMICS APPLIED TO CORIOLIS METERS

The motion of particles in an oscillating fluid has been investigated thoroughly, starting in the late 19th century. In this section, we apply this broad theoretical background to the specific case of multiphase measurement in Coriolis flow meters. Many multiphase applications involve viscous fluids such as soap, oil, and ice cream, but it is useful as a first step to evaluate the effects of bubble or particle motion on measurement of an inviscid flow. This analysis will illuminate the driving forces for decoupled motion and offer insight into the differences between gas/liquid, liquid/liquid, and solid/liquid flows.

3.1 Inviscid particle motion model

We begin with the Euler equations, which are found from the Navier-Stokes equations by neglecting viscosity and heat transfer. Brennen [2] gives a comprehensive overview of the solution of the Euler equations using potential flow theory for translation of a bubble or particle in an unsteady, inviscid, irrotational flow field. The total force on the particle is given by the following expression, where ρ_f refers to the fluid density and τ is the volume of the particle (f subscripts refer to the fluid, while p subscripts refer to the particle, bubble, or droplet).

$$F_{total} = F_{addedmass} + F_{buoyancy} = \frac{1}{2}\rho_f \tau\left(\frac{du}{dt} - \frac{dv}{dt}\right) + \rho_f \tau \frac{du}{dt} \tag{3}$$

Here, u and v are the fluid and particle velocities, respectively. Two forces act on a spherical particle in unsteady potential flow with the stated assumptions. The first force on the right hand side of equation (3) accounts for the added mass effect which is caused by the acceleration of the surrounding fluid due to the spherical particle which is constantly displacing fluid as it moves through the flow field. The second force in (3) is an inertial

buoyancy-like force caused by the acceleration of the fluid relative to an inertial frame. The acceleration of the fluid causes a pressure gradient which produces the force term. This is similar to the force causing a bubble to rise up through water, or a slug of gas to "slip" through a pipeline with superficial velocity. Newton's Law can be applied to obtain a differential equation for particle motion, with the mass of the particle times its acceleration on the left, and the sum of the forces on the right.

$$m_p \frac{dv}{dt} = \frac{1}{2}\rho_f \tau \left(\frac{du}{dt} - \frac{dv}{dt} \right) + \rho_f \tau \frac{du}{dt} \tag{4}$$

Given the definition of particle mass, $m_p = \rho_p \tau$, equation (4) reduces to the following:

$$\left(1 + \frac{2\rho_p}{\rho_f} \right) \frac{dv}{dt} = 3\frac{du}{dt} \tag{5}$$

Equation (5) indicates that for a bubble of negligible density in oil ($\rho_p << \rho_f$), the bubble will have three times the acceleration of the fluid. Integrating the equation twice shows that the particle travels three times as far as the fluid per oscillation of the flow tube, as shown graphically in Figure 5. A droplet of liquid having the same density as the bulk fluid ($\rho_p = \rho_f$) will have the same position, velocity, and acceleration responses as the liquid. If the particle is more dense than the liquid ($\rho_p > \rho_f$), then the liquid will experience greater acceleration than the particle.

The liquid phase is assumed incompressible and generally to move directly with the tube. This ignores some circulation effects that occur because of the tube's circular geometry, the oscillatory motion of the pipe, and the swirl in the pipe caused by the manifold geometry. It is reasonable to neglect these effects because they do not cause changes in the location of the center of gravity of the fluid in the tube, which is the mechanism by which decoupling causes measurement errors. Given these assumptions, the fluid motion will be sinusoidal with angular frequency ω and amplitude A_f, and the particle will in general respond at the same frequency but different amplitude, A_p, and phase delay, φ.

$$\text{Fluid Displacement} = A_f \sin(\omega t) \tag{6}$$

$$\text{Fluid Velocity} = u = \omega A_f \cos(\omega t) \tag{7}$$

$$\text{Particle Displacement} = A_p \sin\left(\omega t + \varphi\right) \tag{8}$$

$$\text{Particle Velocity} = v = \omega A_p \cos\left(\omega t + \varphi\right) \tag{9}$$

It may be intuitively unclear why a bubble moves further than the bulk fluid on each oscillation of the flow tube and why a solid particle moves less. To understand this, consider the simple case of a bubble flowing with a fluid inside a pipe. Relative movement of the gas phase in pipe flow is typically known as the slip velocity, and is a measure of how fast the gas phase moves with respect to the liquid phase. This is similar to the case of decoupling in oscillatory motion, except that the acceleration is caused by a pressure gradient instead of tube motion.

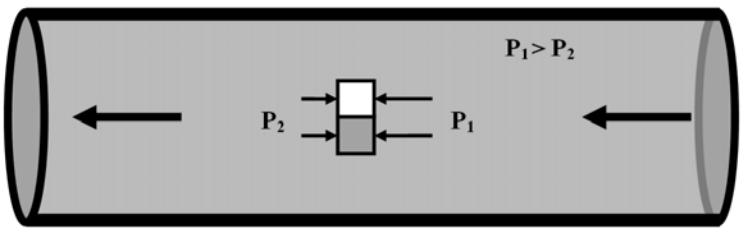

Fig. 10 - Bubble slip velocity in pipe flow

Consider two equally sized cubes of fluid flowing through a pipe as shown in Figure 10. The first cube is

an air pocket and the second is a fluid of the same density as the surrounding fluid. The same pressure force is exerted on the upstream and downstream faces of both cubes, and all pressure forces exerted on faces in the direction perpendicular to flow cancel out. Therefore, with the same pressure force exerted over the same area, each cube will experience the same net pressure force in the downstream direction. Bubble slip occurs because the gas cube is less dense than the liquid cube and Newton's law requires that, under the same force, the lighter gas cube must have higher acceleration. The added mass force resists the relative motion between the gas cube and the liquid cube, but it does not completely stop the motion so long as the gas is less dense than the liquid. As will be shown later, larger bubbles experience larger slip velocities, while highly viscous fluids tend to keep slip velocities low. If the gas cube was instead replaced with a solid cube of greater density than the liquid, the solid cube would move more slowly than the liquid by the same arguments. These same effects occur in the direction of oscillation of a Coriolis meter flow tube and cause the relative motion we call decoupling.

3.2 Viscous particle motion model

In order to predict Coriolis meter performance in a wider range of multiphase flow applications, we extend the potential flow theory to incorporate viscous effects. The viscous model includes two new forces, the drag force and the history, or Basset, force. With the addition of these forces, the decoupling between the particle and fluid decreases, especially at higher viscosity. This is because the drag and history forces impede the decoupled motion between the particle and fluid. We also expect the motion of the particle and fluid to be out of phase because of the lag in deceleration and acceleration of the particle caused by the addition of the drag force.

Modeling oscillatory motion of a sphere through a viscous fluid is complicated. A viscous wake region develops behind the sphere as fluid flows past it and boundary layer separation occurs. For a particle which oscillates back and forth through its own wake, various modifications to the equations of motion must be made in order to correctly predict the physics. The theoretical basis for unsteady motion of a rigid particle in a viscous fluid is usually credited to Basset [3], though others studied the same problem independently. Through solution of the unsteady Stokes equations, Basset determined an expression for particle motion with a no-slip boundary condition, which is essentially the acceleration of a particle of mass $(4/3)\pi a^3\rho_p$ due to the summation of forces acting on the particle. Basset's solution assumed very low Reynolds numbers and a no-slip boundary condition at the surface of the sphere, but more contemporary research has led to improvements to the equation of motion to allow application at a wide range of Reynolds numbers and boundary conditions. The equation of motion for a solid sphere in an oscillating viscous fluid is given by:

$$m_p \frac{dv}{dt} = F_{drag} + F_{history} + F_{addedmass} + F_{buoyancy} \tag{10}$$

Where the force terms are defined as follows:

$$F_{drag} = 6\pi\mu_f a\left(u - v\right)\varphi(\mathrm{Re}) \tag{11}$$

$$F_{history} = 6\pi\mu_f a\left[\frac{u-v}{\delta} + \frac{\delta\rho_f a^2}{2\mu_f}\left(\frac{du}{dt} - \frac{dv}{dt}\right)\right] \tag{12}$$

$$F_{addedmass} = \frac{2}{3}\pi\rho_f a^3\left(\frac{du}{dt} - \frac{dv}{dt}\right) \tag{13}$$

$$F_{buoyancy} = \frac{4}{3}\pi\rho_f a^3\frac{du}{dt} \tag{14}$$

Here, a, ρ_p, ρ_f, μ_f, v, and u are the particle radius, particle density, fluid density, fluid viscosity, particle velocity, and fluid velocity, respectively. On the right hand side of equation (10), the first force term is the Stokes drag law. The Stokes empirical correction factor, $\varphi(Re)$, accounts for deviation from the low Reynolds number formulation. The second term on the right hand side of equation (10) is the Basset or history force which accounts for the effects of the past motion of the particle travelling through its own wake. The inverse Stokes number, δ, represents a ratio of the oscillation time scale to the viscous diffusion time scale. This parameter is extremely important for predicting motion of an oscillating particle, and will be discussed later in detail. The third force term in (10) is the added mass force and the fourth is the buoyancy-like force that arises due to the accelerating reference frame. An excellent modern derivation and discussion of the particle motion equation can be found in Brennen [2,4], along with solutions for alternate boundary conditions.

Assumptions are made in order to apply the theory to actual multiphase flow in a Coriolis meter. Clearly, potential flow theory cannot accurately predict viscous effects, flow tubes do not constitute infinite fluid media, and bubbles or particles can potentially interact with each other during oscillation. However, for the range of conditions found in a Coriolis meter, the various forms of the force terms can be applied with high confidence in their accuracy, at least to the level needed here for formulation of best practices. For a detailed discussion of the assumptions implicit in this analytic model, please refer to Weinstein [5]. The results for decoupling ratio and phase delay between particle and fluid are also verified experimentally using a shaker table and high speed video camera in Weinstein [6].

The time plot in Figure 11 shows that, for the case of a bubble in a mildly viscous fluid such as water or light oil, the bubble oscillates slightly out of phase with the fluid, and at an amplitude approximately two times greater. With the addition of viscous effects to the model, the decoupling ratio decreases from the theoretical maximum of 3:1 down to 2:1, thus improving measurement performance.

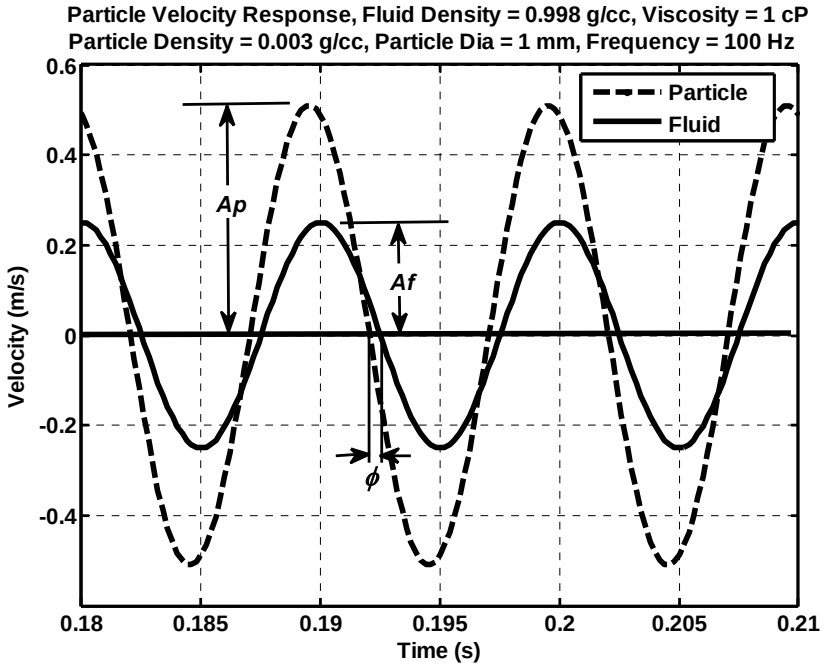

Fig. 11 - Time plot of bubble displacement for viscous model

3.3 Dimensional analysis of the particle motion equation

Nondimensionalizing the equation of motion (10) leads to a deeper understanding of the competing physical effects involved in decoupling. The details of the nondimensionalization are included in Weinstein [5]. Here we include the resulting nondimensionalized equation of motion.

$$\frac{dv}{dt} = \frac{9}{4} R\delta^2 (u-v)\varphi(\mathrm{Re}) + \frac{9}{4} R\delta (u-v) + \ldots \\ \frac{9}{2} R\delta \left(\frac{du}{dt} - \frac{dv}{dt} \right) + R\left(\frac{3}{2}\frac{du}{dt} - \frac{1}{2}\frac{dv}{dt} \right) \tag{15}$$

The following nondimensional parameters are found to fully replace the original seven dimensional variables.

$$R = \text{Density Ratio} = \frac{\rho_f}{\rho_p} \qquad \delta = \text{Inverse Stokes \#} = \sqrt{\frac{2\upsilon_f}{\omega a^2}} \\ \text{Decoupling Ratio} = \frac{A_p}{A_f} \qquad \mathrm{Re} = \text{Reynolds \#} = \frac{2aA_f\omega}{\upsilon_f} \tag{16}$$

The density ratio indicates the importance of the inertial difference between the phases, which is the driving force for decoupled motion. If this parameter is exactly equal to 1.0, as for a pure fluid, there is no decoupled motion. The decoupling ratio, A_p/A_f, is the desired output from the model and describes the extent to which the bubbles or particles move with respect to the surrounding liquid. Recall that if decoupling ratio is near 1.0, then measurements will be accurate, whereas decoupling ratios away from 1.0 result in errors. This term arises in equation (15) when the specific expressions for velocity and acceleration are substituted in, for example, $u = \omega A_f \cos(\omega t)$. The inverse Stokes number is an important parameter which describes the ratio of the oscillation time scale to the viscous diffusion time scale. It represents the time it takes for a disturbance created at the surface of an oscillating particle to diffuse into the surrounding flow field.

It is useful to evaluate the nondimensionalized equation (15) in the limit of low and high inverse Stokes number. Low inverse Stokes numbers occur when kinematic viscosity is low or when particle size or frequency are high. In the limit of low inverse Stokes numbers, we recover the inviscid equation of motion, equation (5), dependent only on the density ratio. Conversely, in the limit of high inverse Stokes numbers, we recover the expected result that the particle moves exactly with the fluid on each oscillation, $u = v$.

The final nondimensional parameter is the standard Reynolds number defined in terms of the fluid velocity. This parameter appears in the correction to the Stokes drag law and renders the equation of motion nonlinear. The standard Reynolds number has only a limited impact on the decoupling ratio as compared to the inverse Stokes number or density ratio.

Figure 12 gives results for decoupling ratio for density ratios between 0.1 and 1000, covering the entire range of possible conditions in oil and gas applications, including solid particles and gas bubbles. The (A), (B), and (C) markers refer to specific application examples discussed in Sections 4.1, 4.2, and 4.3, respectively. Increasing the inverse Stokes number moves the decoupling ratio closer to 1.0, indicating a reduction in relative motion. As the density ratio increases past about 50, the decoupling ratio is dependent primarily on the inverse Stokes number. This is especially important because all gas/liquid mixtures have high density ratios, usually above 100. Thus, for the most common multiphase flow conditions in a Coriolis meter, the extent of measurement error depends primarily on the inverse Stokes number. If this parameter is very small, we approach the inviscid case of 3:1 decoupling ratio, while if the parameter is large, relative motion is restricted and the decoupling ratio approaches 1:1.

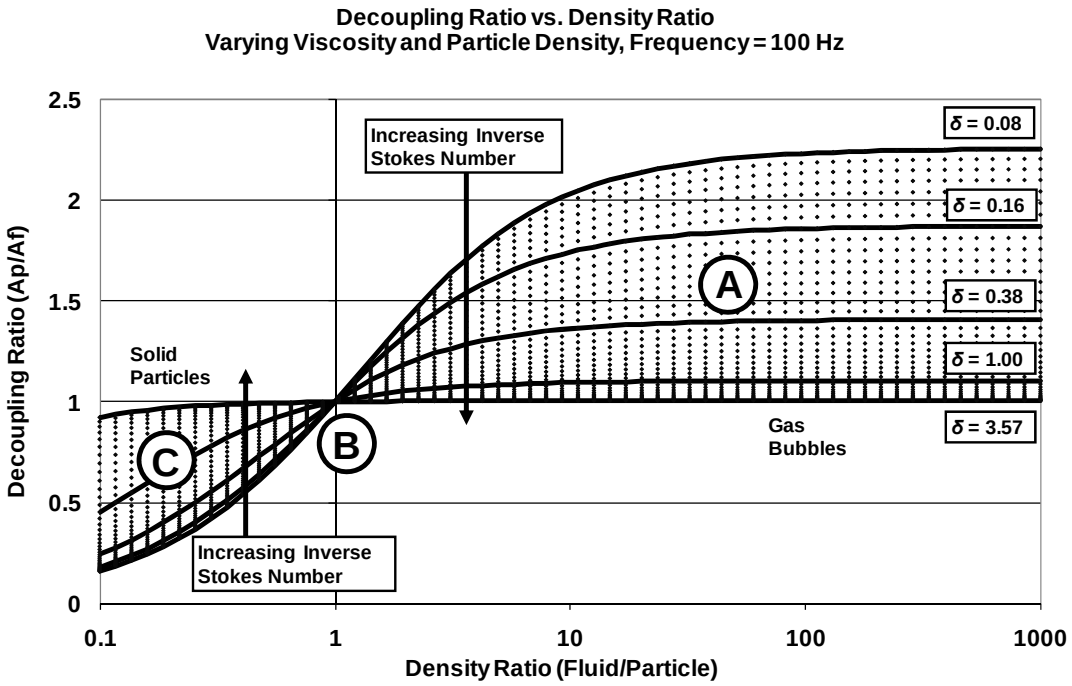

Fig. 12 - Decoupling ratio vs. density ratio, changing δ

The inverse Stokes number, δ, shows that it is the balance between fluid kinematic viscosity, particle size, and frequency that is important, not any one of these variables alone. Because bubble size is the only variable that is squared in δ, small changes in bubble size overwhelm changes in viscosity or frequency. Tests in which we steadily decrease bubble size by increasing turbulent mixing upstream of the meter using a ball valve consistently show improved accuracy in all measurements, regardless of the type of Coriolis meter used.

In the next section, we examine three common oil and gas applications for Coriolis meters – live oil with entrained gas, net oil and watercut, and cementing or drilling. In each case, we apply the theory of decoupling discussed above to establish best practices for successful operation of meters.

4 EXAMPLES OF DECOUPLING IN OIL AND GAS OPERATIONS

Coriolis meters are used extensively in oil and gas applications in which multiphase flow is present. In this section, we use the decoupling theory developed in the previous section to understand sources of error in three completely different O&G applications. In each case, we can significantly improve measurement performance by following a few simple best practices.

4.1 Live Oil Applications with Gas Breakout (A)

One of the most widespread metering challenges of live oil applications is the presence of natural gas. Depending on the pressure and temperature, the natural gas may be in liquid or gas phase, and can be dissolved in the oil or broken out into bubbles or slugs of various sizes. When gas breakout occurs in a Coriolis meter, errors due to decoupling can occur. The magnitude of the error depends primarily on the inverse Stokes number, as discussed in Section 3. The density of oil is typically between 0.8 and 1.0 g/cc, while the density of gas varies significantly with pressure between 0.001 and 0.1 g/cc. The resulting fluid to gas density ratio is between 10 and 1000. Recall that Figure 12 shows that the decoupling ratio is roughly constant over these density ratios (see marker A), but the inverse Stokes number can dramatically impact decoupling ratio, and thus meter performance. For small δ, the decoupling ratio can approach the theoretical maximum of 3:1, and for large δ, the decoupling

ratio reduces to 1:1, resulting in no measurement error. The magnitude of δ is determined by the ratio of kinematic viscosity to the product of frequency and bubble size squared:

$$\delta = \text{Inverse Stokes \#} = \sqrt{\frac{2\upsilon_f}{\omega a^2}} \tag{17}$$

In order to use a Coriolis meter in live oil applications with entrained gas, it is critical to ensure that the inverse Stokes number is maximized. This can be accomplished by increasing the viscosity, decreasing tube vibration frequency, or decreasing bubble size. While the oil viscosity is usually not under the user's control, the other two parameters can be optimized by following best practices. Low frequency Coriolis meters are less prone to decoupling errors and should be used when gas entrainment is expected. This is also true for velocity of sound errors, which are minimized when tube frequency is low. Bubble size is squared in the equation for inverse Stokes number, and thus has the most pronounced effect on performance. Increasing pipeline pressure by adding a pump will decrease bubble size, and in some cases eliminate entrained gas entirely. Also, keeping pipeline velocities high and using mixing devices can effectively decrease bubble size and dramatically improve measurement performance. However, this can be a self-defeating practice, because additional gas can break out at high flow rates due to additional pressure drop across the meter. Fortunately, bubble size is typically very small with this type of gas breakout, especially when void fraction is low.

Extensive testing has shown that the best measurement performance is realized when flow rates are kept above a 5:1 turndown from "nominal," where nominal rate is defined as the flow rate at which 1 Bar pressure drop occurs with water. For example, if a water flow rate of 500 lb/min results in 1 Bar pressure drop for a particular meter, the meter should run above 100 lb/min in multiphase applications to ensure that bubbles flush out of the meter properly. For much higher viscosity fluids, for example fuel oil, this recommendation can be pushed to 10:1 turndown because viscous effects ensure that bubbles are dragged out of the flow tubes. In live oil applications, special care should be taken as a well matures, as flow meters are often sized for peak production. When a well nears the end of its life, a dump cycle can be used to keep pipeline velocities high.

Figure 13 shows the influence of fluid viscosity and bubble radius on the density error expected in a 100Hz Coriolis meter with a density ratio representative of that found in a live oil application. Note that density error is defined as the percentage deviation from true mixture density. The derivation of an analytical expression for density error due to decoupling in a Coriolis meter can be found in Weinstein [5]. Density errors are reported here because of the availability of a closed-form expression, however testing has shown that similar trends exist for mass flow.

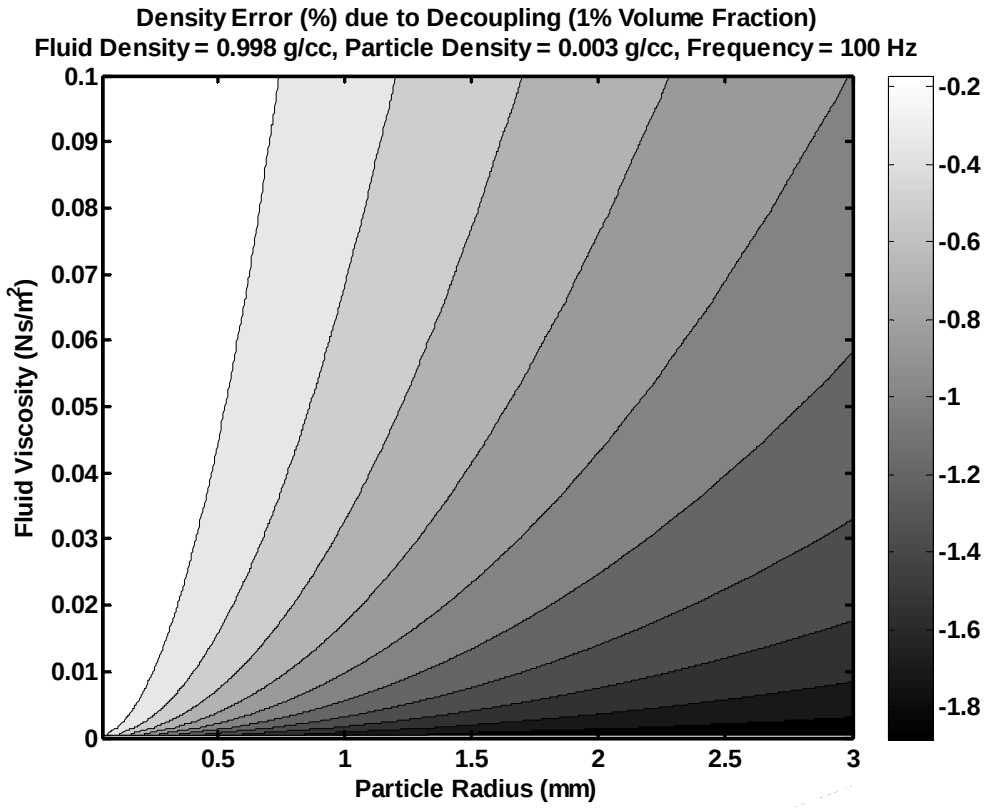

Fig. 13 – Density error as a function of fluid properties

As shown in the figure, errors in a live oil application can vary significantly depending on the value of the inverse Stokes number. For best performance, ensure that the fluid mixture is homogeneous with small bubble sizes, and use a low frequency Coriolis meter if possible.

4.2 Net Oil and Watercut Measurement (B)

Net oil measurement with a Coriolis meter allows a user to simultaneously determine watercut, oil flow rate, and water flow rate from a single device. The meter provides mixture density and mass flow measurements, which can be used along with known base densities for water and oil to determine the unknown water and oil volume fractions.

$$\begin{aligned} &\rho_m = \rho_w \phi_w + \rho_o \phi_o \\ &\phi_w + \phi_o = 1 \\ &\dot{q}_o = \dot{q}_m \phi_o \quad ; \quad \dot{q}_w = \dot{q}_m \phi_w \end{aligned} \tag{18}$$

Here, the (*m*), (*w*), and (*o*) subscripts represent “mixture”, “water”, and “oil” quantities, respectively. The density of the oil and water are known in advance, and the Coriolis meter provides mixture density, ρ_m, and mixture flow rate, q_m. The first two equations are solved simultaneously for the oil and water volume fractions, φ_o and φ_w, and the oil and water flow rates are then calculated using the known volume fractions. The flow rate can be either a volume or mass flow rate, as a Coriolis meter can measure both.

Error due to decoupling is usually negligible for net oil applications because the density ratio is so close to 1.0. Recall from Figure 12 that a density ratio near 1.0 results in a decoupling ratio that is also near 1.0 (see marker B). For a mixture of two fluids with the same density, the density ratio is exactly 1.0 and decoupling errors do not occur because there is no buoyant force to cause the relative motion between the two fluids. With a density of 1.0 g/cc for water and 0.85 g/cc for oil, the density ratio for a net oil application is 1.18. At a density

ratio of 1.18, the error due to decoupling is negligible as long as the flow rate is high enough to keep the water and oil moving through the meter.

For net oil applications, it is recommended that the meter be operated at flow rates above 20:1 turndown from nominal, where nominal rate is defined as the flow rate at which 1 Bar pressure drop occurs with water. As with live oil applications, special care should be taken as the well matures, as flow rates drop well below peak production levels. At extremely low flow rates, it is possible to "hold up" oil or water inside the flow tubes, which results in an artificially high or low net oil measurement because the meter simply measures the density of the mixture currently inside the flow tubes. If some oil gets stuck on the inlet side of the meter, then the meter will register a lower mixture density than the density representative of the actual pipeline, and will over-report oil production. Another similar issue is pipeline "slip" velocity, discussed at the end of Section 3.1, which occurs when the oil phase moves faster than the water phase through the pipeline. For net oil applications, these issues can be completely avoided by proper meter sizing to ensure a well-mixed fluid. This topic was investigated experimentally by TUV NEL and presented at a prior North Sea Workshop [7].

So far, we have only considered net oil applications in which water and oil are the only components present in the pipeline. When gas bubbles are present, the Coriolis meter correctly measures the lowered mixture density, ρ_m. However, the reduction in density is misinterpreted by the net oil equations (18) as an increase in oil output. Because the density of the gas is so low, even a small amount of gas can represent a large amount of oil. For example, consider a mixture of water and oil with 50% volume fraction of each component. If the density of water and oil are 1.0 g/cc and 0.8 g/cc, respectively, then the Coriolis meter will measure 0.9 g/cc and the net oil equations will output 50% watercut. However, if 5% gas volume fraction is added to the mixture, then the Coriolis meter will again measure the correct mixture density, now roughly 0.85 g/cc, but the net oil equations will indicate 75% watercut even though the true watercut is 50%.

Coriolis meters offer extremely accurate measurements in net oil applications, so long as the meter is properly sized and entrained gas is avoided. When occasional gas is unavoidable, the Coriolis meter provides a robust detection capability, tube excitation power, as discussed in Section 5. This enables the user to confidently use the net oil outputs from a Coriolis meter when conditions are stable, and quickly identify and fix problems with separators or other equipment when process upsets occur.

4.3 Cementing and Drilling Mud Applications (C)

Many oil and gas applications involve particle-laden fluids, such as cement, drilling mud, or fracture sand. The decoupling models described in Section 3 are equally applicable for solid particles as for gas bubbles, and the mechanism for measurement error is the same - decoupling. A solid particle is typically denser than the fluid, so it moves to a lesser extent on each oscillation cycle than the surrounding fluid. This causes the center of gravity to move backwards with respect to the center of the tube (ie. the center of gravity of the fluid mixture inside the tube moves less far than the center of the tube). This also occurs in the case of a gas bubble, which moves further on each oscillation than the surrounding fluid, but because the surrounding fluid is heavier than the bubble, the shift in center of gravity is still backwards with respect to the direction of oscillation. For this reason, measurement errors due to decoupling are negative regardless of the density of the inclusion.

Consulting Figure 12 for density ratios of less than 1.0 (see marker C), we again find that decoupling ratio is further from 1.0 for density ratios further from 1.0. Also, decoupling ratio is further from 1.0 when inverse Stokes number is small. Therefore, the same recommendations from live oil and net oil applications still apply. Lower frequency Coriolis meters will outperform higher frequency meters because decoupling is reduced, and small sand or rock sizes will result in dramatically improved performance over large sizes. Experimental results from a fracture sand test verified the influence of both of these factors, frequency and sand size. The best density measurement was found using a low frequency Coriolis meter on the smallest sand size. On the other hand, performance was unacceptable using a high frequency Coriolis meter, with small or large sand sizes.

5 MULTIPHASE DETECTION USING TUBE EXCITATION POWER

In many oil and gas applications, entrained gas is an unexpected process upset that is avoided under normal operating conditions. For example, custody transfer of pipeline quality oil, or allocation measurement downstream of a separator. Coriolis meters provide an extremely useful diagnostic output, tube excitation power, which can be used as an indicator of entrained gas or solid particles in the process fluid. For example, tube excitation power can be monitored to keep a separator's level at the proper height for optimal separation.

The Coriolis flow meter relies on limited power to maintain tube oscillation. The flow tubes are driven on resonance in the first bend mode, so very little energy is needed to keep the tubes oscillating. In fact, the structural damping in a Coriolis meter is minimized during the design process so that excitation power is low enough to meet safety regulation limits. The low power requirement is usually not an issue because single phase liquids and gases do not significantly increase damping of the flow tubes. Increasing viscosity causes only slight increases in energy requirements.

On each oscillation, the tube does a certain amount of work on the fluid. For single phase flows, very little work is required to keep tubes oscillating. However, when multiple phases are present, much of the input energy is used to create the relative motion between the particles and the fluid we call decoupling. As shown in Figure 14, the drive power required increases dramatically with gas entrainment until the maximum allowable values for voltage and current are reached. This occurs at surprisingly low void fractions, generally around one percent as determined from testing of Coriolis meters with entrained gas. If additional power dissipation occurs, for example by the addition of more gas, then the amplitude of tube vibration begins to decrease because drive power is limited.

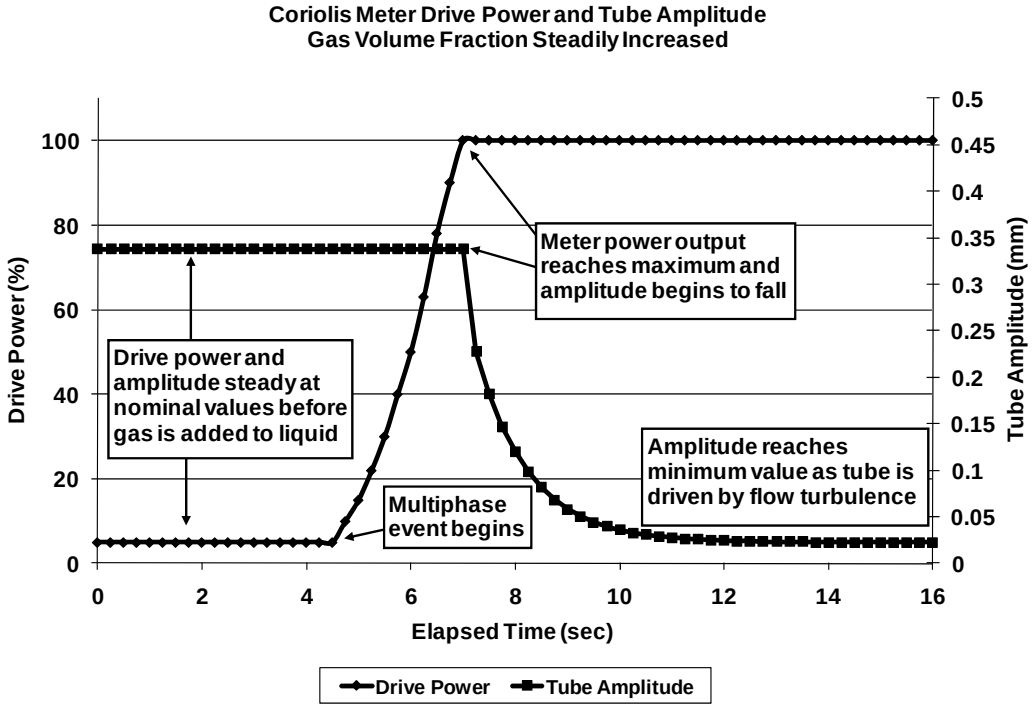

Fig. 14 – Drive power and tube amplitude response during multiphase event

With increasing gas entrainment, the tube amplitude eventually reaches a minimum value for which the turbulence in the flow actually keeps the tubes vibrating. If signal processing algorithms are carefully designed, it is possible to continue measuring accurately at very low amplitudes, although the signal to noise ratio is low and measurements can be noisy.

Increased drive power is a very useful indicator of entrained gas or solid particles, however it cannot be used to predict how much measurement error is occurring due to multiphase effects. The reason for this is that drive power is far more dependent on the phase difference between the particle and the fluid, rather than the amplitude ratio. Still, for most applications, a reliable detection of entrained gas is the most critical requirement.

6 BEST PRACTICES AND CONCLUSIONS

Understanding of the sources of error in a Coriolis meter in multiphase flow is improving, although complete compensation for decoupling errors is unlikely due to the complexity of the physics and the fact that bubble size is generally unknown. These challenges also make it difficult to predict exact measurement error magnitude for specific applications. However, extensive testing has shown that Coriolis meters perform well in multiphase applications in which certain conditions are met, and frequently outperform other flow measurement technologies, such as volumetric meters, which over-report liquid-only quantities due to the increased flow volume associated with bubbly mixtures. In addition, Coriolis meters provide a dependable diagnostic for detection of entrained gas or solid particles in a fluid, which can be used to quickly fix process problems such as poorly tuned separators or leaking pump seals.

Trends for decoupling and other errors discussed in this paper allow for better recommendations to users regarding how to install and operate Coriolis meters when multiple phases are present. Dimensional analysis of the particle motion equation yields several important parameters, including the density ratio and the inverse Stokes number. Analysis of these parameters explains Coriolis meter performance in diverse multiphase applications, such as live oil, watercut measurement, and fracture sand operations.

Assuming that fluid properties are pre-defined for a given application, the most important operational practices for achieving good performance with a Coriolis meter are (1) choosing a low frequency Coriolis meter for multiphase applications, (2) minimizing bubble or particle size through mixing and increased pressure, and (3) keeping flow rates high enough to prevent holdup and flow tube asymmetry.

Future Coriolis meter design improvements can be made by reducing drive frequency, as a very low frequency meter would be essentially immune to multiphase effects, including decoupling and velocity of sound. While complete compensation of multiphase errors in a Coriolis meter may never be possible, following a set of simple guidelines is effective for reducing measurement errors to acceptable levels. With these best practices, Coriolis meters will remain a leading solution for inline measurement of process fluids prone to small amounts of entrained gas or solid particles.

3 NOTATION

a	Particle radius
A_f	Amplitude of fluid oscillation
A_p	Amplitude of particle oscillation
c	Velocity of sound
d	Tube diameter, VOS model
$f_{(sub)}$	Subscript indicates “fluid”
F_c	Coriolis force
$m_{(sub)}$	Subscript indicates “mixture”
m_p	Mass of particle
$p_{(sub)}$	Subscript indicates “particle”
R	Fluid to particle density ratio
Re	Reynolds number
u	Velocity of fluid
v	Velocity of particle
δ	Inverse Stokes number
μ_f	Dynamic viscosity of fluid
v_f	Kinematic viscosity of fluid
ρ_f	Density of fluid
ρ_m	Density of mixture
ρ_p	Density of particle
τ	Volume of particle
φ	Phase angle, particle vs. fluid
φ	Component volume fraction
$\varphi(Re)$	Correction to Stokes drag law
ω	Angular frequency fluid oscillation

4 REFERENCES

[1] J. HEMP AND J. KUTIN. 2006. Theory of errors in Coriolis flowmeter readings due to compressibility of the fluid being metered. *Flow Measurement and Instrumentation*. 17:359-369.

[2] C.E. BRENNEN. 1995. Cavitation and bubble dynamics. *Oxford University Press*, New York.

[3] A.B. BASSET. 1888. Treatise on hydrodynamics. *Deighton Bell*, London.

[4] C.E. BRENNEN. 2005. Fundamentals of multiphase flow. *Cambridge University Press*, New York.

[5] J.A. WEINSTEIN. 2008. The motion of bubbles and particles in oscillating liquids with applications to multiphase flow in Coriolis meters. *University of Colorado at Boulder Dissertation*. Proquest: AAT 3315790.

[6] J.A. WEINSTEIN, D.R. KASSOY, AND M.J. BELL. 2008. Experimental study of oscillatory motion of particles and bubbles with applications to Coriolis flow meters. *Physics of Fluids.* 20.

[7] O. ANDERSON, G. MILLER, R. HARVEY, AND D. STEWART. 2004.Two component Coriolis measurement of oil and water at low velocities. *North Sea Flow Measurement Workshop*. Paper 7.3.

North Sea FLOW Measurement Workshop

Paper 7.3

Use of Dual-Modality Tomography for Complex Flow Visualisation

Norman Glen
TUV NEL

Amy Ross
TUV NEL

TÜV SÜD

nel technology for life

28th International North Sea Flow Measurement Workshop
26th – 29th October 2010

Use of Dual-Modality Tomography for Complex Flow Visualisation

Norman Glen, TUV NEL
Amy Ross, TUV NEL

1 INTRODUCTION

The development of new flow metering techniques and the use of existing flow meters in more challenging applications requires more data than just bulk flow calibration measurements. The flow structure and its impact on the meter performance are vital pieces of information, without which the value of experimental research data can be limited. This is particularly true for complex flow characterisation.

With the development of more sophisticated technologies to measure increasingly complex flows there is a need for additional knowledge of flow patterns in National Standard flow facilities, as well as accurate measurement of the individual phases which constitute the multiphase mixtures.

Tomography systems have developed rapidly over the last 10 years, culminating in the recent development of multi-modal tomographic systems which are aimed at overcoming some of the limitations of single-modal systems. The UK is the leading centre for industrial process tomography in the world; whilst the pharmaceutical sector is already firmly engaged with the technology and reaping benefits, more general uptake has been limited. However, there is a need to develop tomography systems that will provide the capability to image complex multiphase flows, such that fundamental research can be undertaken on detailed flow structure phenomena, and how they relate to multiphase measurement performance. This is particularly timely in view of developments from several flow meter manufacturers.

As part of the 2008-2011 Engineering and Flow Programme for the UK's National Measurement Office, TUV NEL Ltd carried out an evaluation of commercially-available tomography systems to assess their suitability for use in flow standard facilities. The successful implementation of a tomographic flow characterisation capability would improve the capability of the UK national multiphase flow measurement facilities [1, 2] and help the facilities keep pace with new and emerging requirements for flow measurement of complex fluid systems, like that for high viscosity multiphase flows. Much of the research performed on these facilities would benefit from the ability to fully understand the fluid dynamics and flow structures. In addition, the use of modelling as a predictive tool in complex flows is well established, and the ability to visualise a real flow stream would have a major impact on the validation of modelling software, allowing users to have confidence in the use of the codes in more challenging flow systems.

2 BACKGROUND

No longer is oil extracted as a single phase, instead it arrives at the well head along with water, gas, sand, waxes, and other fluids used for well optimisation such as glycols. This has driven the need for better understanding of flow regimes and phase interactions.

Multiphase meters use mathematical models to try and predict the flow regime they are encountering at any moment in time. Getting the answer wrong can lead to significant over or under reading [3]. Many multiphase meters are installed vertically as this reduces the number of potential flow patterns from seven (stratified, stratified wavy, plug, slug, bubble, annular and mist) to four (bubble, slug, churn and annular). Often a blinded tee is installed directly upstream of the meter in an attempt to remove slip and homogenise the flow but this does not always work. As the world moves into an era where oil supplies are becoming more viscous, flow patterns are changing meaning a greater understanding of them is required.

The determination of flow regimes in pipes is not easy. Some techniques used include analysis of fluctuations of local pressure and/or density or by direct visual observation if a length of transparent pipe is installed in the line. This means that depending who is interpreting the results or looking at the pipe, one can get different answers. What one observer may classify as slug flow could be considered as plug flow if viewed by someone else. This means that descriptions of flow regimes are to some extent arbitrary [4].

A major source of error in multiphase flow metering is fluid properties. Over the course of its lifetime, the fluids coming from the well change, meaning the fluid properties will also change. Sampling is used to combat this so that the fluid properties being used by the meters can be updated. But how representative is the sample? Where should it be taken from? A technique enabling one to see inside the pipe, used in conjunction with sampling, will give more confidence in the samples collected, therefore more confidence in the fluid properties, leading to more confidence in the meter readings. In principle, tomography is a suitable technique to provide visualisation of what is happening inside a pipe.

Tomography is a technique for displaying a cross section through an object. Tomographic measurement technologies involve the acquisition of measurement signals from sensors located external to the object under investigation. It is necessary to gather projection data from multiple directions which is then processed by an image reconstruction algorithm to produce a tomographic image. This can achieved by rotating the object within the sensor field or rotating the sensors around the object. Tomography is perhaps most associated with medical imaging as illustrated by techniques such as Computed Tomography (CT) which uses rotating X-ray sources and detectors and Magnetic Resonance Imaging (MRI) which uses a powerful magnetic field. In both cases, the sensors can rotate at high speed around the human body thereby delivering the necessary projection data from multiple directions. The sensor can also scan in the orthogonal direction allowing a full 3D image to be obtained.

However, it may not always be possible to rotate the object or the sensors due to physical constraints or because the time required may exceed the time available due to time-dependent effects associated with the object under investigation. This is particularly the case with process tomography where the processes under investigation are often changing rapidly, for example, multi-phase flow.

3 DUAL-MODALITY TOMOGRAPHY

The defining feature of any tomographic measurement technology is the sensor system that is deployed. There are a number of sensor systems available based on transmission, acoustic and electrical technology and the key to determining which system is appropriate is to consider the properties of the process that can be exploited to deliver the required information. Most tomographic measurement technologies employ a single sensor system and this does limit the range of potential applications. Table 1 summarises various tomography techniques that can be applied to process applications [5].

Electrical tomographic measurement techniques are suitable for imaging multi-phase flow processes. The attributes associated with these techniques are high temporal resolution, ability to operate in opaque systems and generally low-cost (certainly when compared to radioactive tomographic techniques). Electrical Resistance Tomography (ERT) exploits differences in conductivity (or resistivity) within the sensing space and Electrical Capacitance Tomography (ECT) exploits differences in electrical permittivity. Individually, these techniques are popular for studying 2-phase flow processes. In the case of ERT it is necessary for the continuous phase to be electrically conducting such as in hydraulic conveying (liquid-solid flow), [6 - 7]. On the other hand, ECT works best with non-conducting materials (or at least where the continuous phase is non-conducting). Popular applications of ECT include pneumatic conveying [8], fluidised beds [9] (both gas-solid systems) and oil continuous flow, [10 -11] (oil-gas systems).

Table 1 - Tomography Techniques for Process Applications

Principle	Spatial Resolution (% of diameter of cross-section)	Practical Realisation	Comment
Electro-magnetic Radiation	1%	Optical	Fast Optical access required
		X-ray and γ-ray	Slow Radiation containment
		Positron emission	Labelled particle Not on-line
		Magnetic resonance	Fast Expensive for large vessels
Acoustic	3%	Ultrasound	Sonic speed limitation Complex to use
Electrical Properties	10%	Capacitance Resistance Impedance	Fast Low Cost Suitable for large or small vessels

Electrical capacitance sensors have been used to measure the component fraction of multi-component flow processes [12]. In this application, the sensors consist of two electrode plates and the capacitance measured is determined by:

$$C = K\varepsilon_m \tag{1}$$

In order to improve the measurement quality of such systems, the size of the electrodes can be increased since the measured capacitance is proportional to the electrode surface area. The requirements for tomographic imaging are different since projection data must be gathered at multiple directions. This is achieved by arranging multiple electrodes around the boundary of the region and the capacitance between all the combination pairs of the electrodes should be measured. Typically twelve electrodes are mounted on the periphery of an insulating pipe with an overall outer earthed screen as shown in the schematic of an ECT sensor in Figure 1(a). This arrangement has the advantage that the electrodes are not in contact with the fluid inside the pipe so the sensor is non-intrusive and non-invasive. The capacitance between all independent pairs of electrodes is measured using a stray-immune circuit which is insensitive to the stray capacitances between the selected electrode and the redundant electrodes and those between the selected electrode and earth. This involves applying an alternating voltage (typical frequency = 1 MHz) from a low impedance supply to the selected electrode. The detection electrodes are all earthed and the current is measured sequentially on each of these electrodes. The second electrode is then selected and the sequence is repeated until all independent pairs of electrodes have been measured.

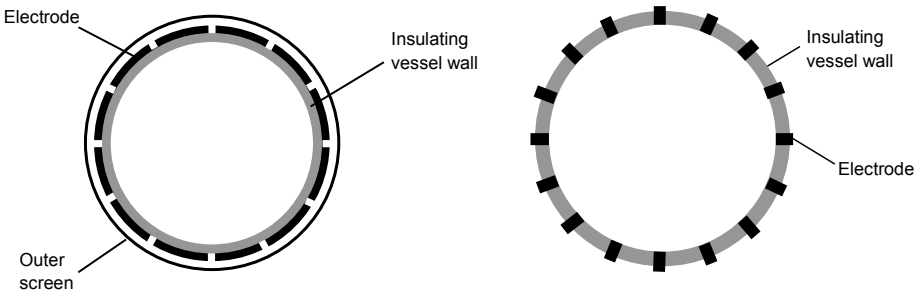

Fig. 1 - Sensor schematic - (a) ECT and (b) ERT

An ERT sensor consists of multiple point electrodes on the periphery of a pipe as illustrated in Figure 1(b). As with ECT, the electrodes are positioned equidistantly around the periphery but unlike ECT they make contact with the fluid inside the pipe. The electrodes are usually

designed to be flush with the vessel wall so that the technique is considered invasive but non-intrusive. An alternating current (typical frequency = 10 KHz) is applied to a source and sink electrode and the generated voltages between other electrodes pairs measured according to a pre-defined measurement strategy. The injection pair is changed and other measurements taken until all independent measurements for the particular strategy have been taken.

In order for a tomographic measurement device to be suitable for imaging flows where the continuous phase may be electrically conducting (water) or electrically non-conducting (oil) it is necessary to deploy both ERT and ECT. This was the main driver behind the development of the dual-modality electrical tomography system. This system originated from the UK Government's Office of Science and Technology Foresight Challenge Project 'Process tomography - a new dimension in advanced sensor technology' (EPSRC Ref **GR/L37434/01),** which ran from 1997 to 2001 involving the Universities of Manchester, Leeds and Exeter and 10 companies. The hardware and software developed during the project were later licensed and then commercialised.

Hoyle et al. [13] discusses the design concept of the multi-modal tomography system and highlights the primary identified application area of multi-phase flow. Multi-modality systems inherently encourage a systematic approach in contrast to current single modality tomographic systems that are complex, expensive and designed primarily for laboratory use. A successful multi-modality system must allow individual sensor data to be collected and combined effectively and it must exploit opportunities for rationalization and sharing of resources, and deal with hazards of mutual interference. The platform proposed by Hoyle et al. [13] supports capacitance, resistance and ultrasound modalities although only capacitance and resistance were used in this study.

4 TECHNICAL APPROACH

4.1 The TUV NEL Multiphase Flow Facility

The TUV NEL multiphase facility consists of a three-phase separator and test loop section (Figure 2). The oil is supplied from the separator to the main oil pump and then to the oil flow metering section. A side-stream sampling loop and a main bypass loop are fitted on the delivery side of the pump. The same configuration exists on the water side.

The bypass loops permit control over the pressure and flow rates of the phases in the test section. The sampling loops provide information on any cross contamination in the oil and water process streams. Heat exchanger circuits stabilise the temperature of the working fluid, which is generally kept between 40°C and 42°C during tests.

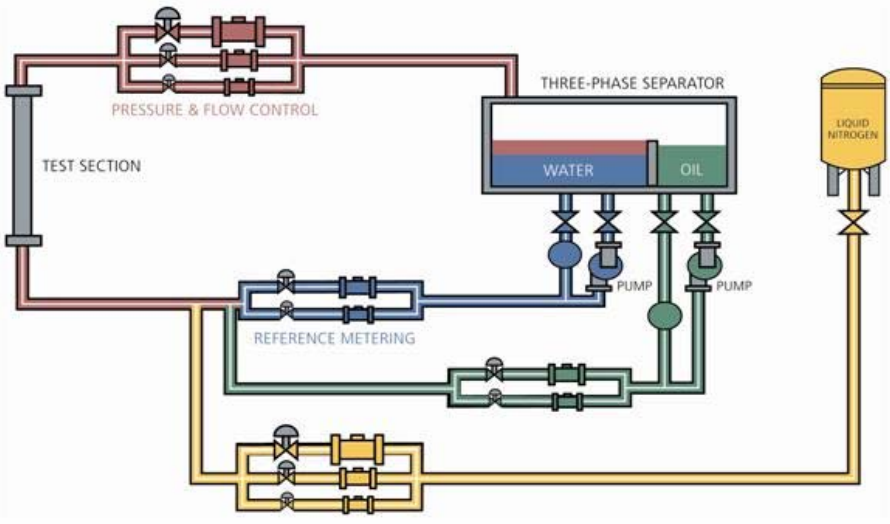

Fig. 2 - TUV NEL multiphase test facility

The oil and water pass through the reference metering stage and are then combined in the mixing section. The nitrogen, which is produced from a liquid nitrogen supply tank external to the building, is injected into the test section after passing through the gas reference metering section. The mixture in the test section runs horizontally to the test meter. Downstream, control valves are used to control the test section pressure. The flow then returns to the separator where the oil and water are separated, and the gas exhausted to atmosphere.

The oil used in the test loop is a mixture of stabilised Forties/Oseberg crude and Exxon D80. The oil phase has a density of around 867 kgm^{-3} at 20°C. The oil viscosity is approximately 23cP at 20°C and 9cP at 40°C. The water phase is a magnesium sulphate solution with an adjustable salinity/density.

4.2 The Dual-Modality Tomography System

Only one potentially suitable tomography system was identified for evaluation. This dual-modality electrical tomography system comprises two integrated modules; electrical resistance tomography and electrical capacitance tomography operated by a single software interface. A dual-modality sensor was designed and fabricated in accordance with the Pressure Systems Directive (97/23/EC) as shown in Figure 3. The sensor was made from a 5" Nominal Bore section of steel pipe connected to 4" Class 150 flanges. The pipe was lined with PVDF (Polyvinylidene Fluoride) to match the bore of the 4" pipe at the NEL Multi-phase flow facility. The 12 ECT electrodes are located within a cavity between the PVDF linear and the steel pipe). The 16 ERT electrodes are located around the external continuous ring welded to the pipe to provide pressure integrity.

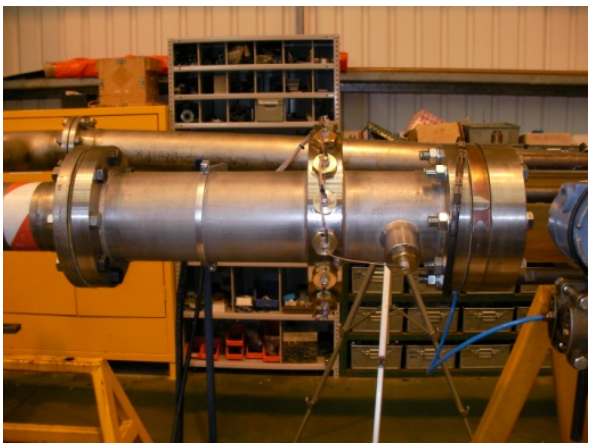

Fig. 3 - Dual-modality sensor

The dual-modality electrical tomography system is capable of operating a maximum of 32 ERT electrodes arranged as with sensors having 8, 16 or 32 electrodes and a maximum of 24 ERT electrodes with sensors having 8, 12 or 24 electrodes. The ECT module utilises an ac-based sinusoidal excitation method which produces good signal to noise performance and the ERT module produces sinusoidal currents to excite a pair of electrodes and the resulting potential difference is measured between other pairs of electrodes.

The software enables the design of flexible excitation strategies for both modalities. In this study a conventional ECT strategy was employed whereby the capacitance was measured between electrodes 1-2, 1-3, 1-4, …., 1-12, then 2-3, 3-4, …., 2-12 until finally 11-12. For a 12-electrode ECT sensor there are 66 capacitance measurements when this strategy is followed. The adjacent strategy was used for ERT whereby current is injected between an adjacent pair of electrodes (e.g. 1-2) and then the potential difference is measured between all other adjacent pairs not including the excitation pair (3-4, 4-5, 5-6, 6-7, 7-8). For an 8-electrode ERT sensor there are 24 independent measurements according to this strategy.

4.3 Imaging Equipment

4.3.1 Direct Visual Observation

During the test programme a Perspex viewing section was installed directly upstream of the tomography system to enable visual observation of the multiphase flow patterns generated. The flow patterns observed were recorded in High Definition using a JVC Everio GZ-HD7 HD Camcorder.

4.3.2 Gamma Densitometer

In fluid flow measurement, gamma densitometers are often used to calculate fluid densities, interface level and slug frequencies. A gamma densitometer was installed immediately downstream of the tomography spool. The densitometer functions by emitting a beam diametrically across the pipe to a detector. This essentially measures the height of the liquid-gas interface rather than the cross-sectional area of the pipe filled with liquid or gas. Consequently, the measured density differs slightly from the actual average density in the pipe.

4.4 Test Programme

The dual-modality tomography system was initially installed horizontally in a straight section of the flow loop (Figure 4a and 4b). In this set up, gravity produces separation of the liquid and gas phases, which can in turn leads to phase slip and localised liquid hold-up.

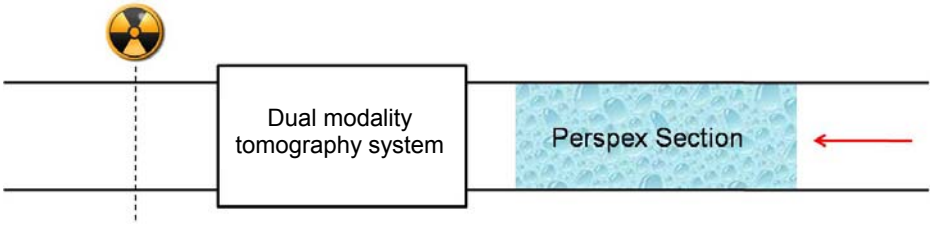

Fig. 4a - Horizontal test set up

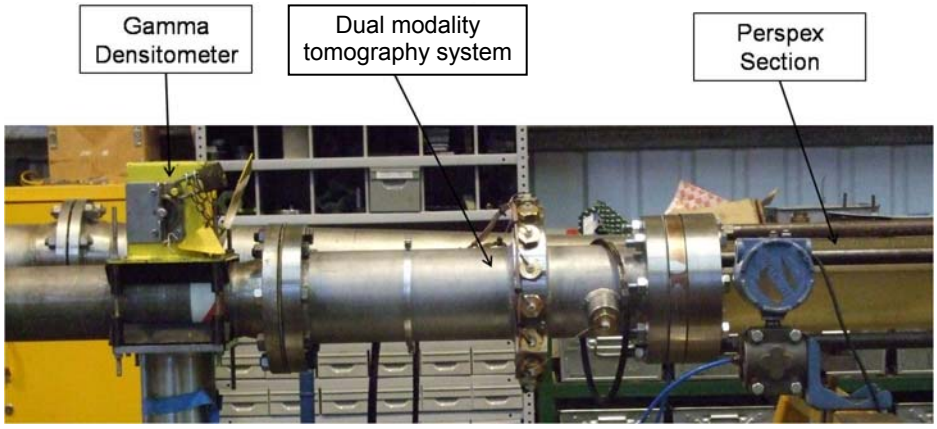

Fig. 4b - Photograph of horizontal test set

On completion of the horizontal tests, the tomography system was installed in a vertical orientation directly downstream of a blinded tee with vertical up-flow, as shown in Figure 5. Many multiphase flow meters are installed this way in an attempt to homogenise the flow and remove/reduce slip. Flow visualisation testing could help quantify how successful using a blinded tee actually is.

4.4.1 Test Matrices

The nominal test matrix developed to cover the three-phase flow map of interest in horizontal flow is shown in Table 2. In addition to covering the range of liquid flowrates and gas volume fractions (GVFs) specified, the test programme intended to cover water cuts of 0, 5, 25, 40, 50, 60, 65, 75, 90, and 100%.

The nominal test matrix developed to cover the three-phase flow map of interest in vertical flow is shown in Table 3. In addition to covering the range of liquid flowrates and GVFs specified, the test programme intended to cover the same water cuts as for the horizontal tests.

The aim of the test matrices was to see how the dual-modality tomography system would cope with a full range of test conditions achievable in the multiphase facility. The most common horizontal flow patterns encountered in the TUV NEL multiphase test loop are bubble and slug, with some stratified and wavy stratified at very low flow rates whilst the most common vertical flow patterns are slug and churn, with annular at high gas flow rates with low liquid content.

Fig. 5 - Vertical test set up

4.4.2 Procedures

For each test run, the flow loop was set up for the required conditions (pressure, temperature, and flow rates) and allowed to stabilise for several minutes.

Test points were initially run from 2 to 10 minute intervals to find the best length for evaluating the system. From these tests it was decided that logging both the multiphase reference instruments and the dual-modality tomography system for 5 minutes at a time was the most suitable option. Video footage was captured during the data collection period where appropriate.

Table 2 - Nominal Two-phase Gas-liquid Test Matrix for Horizontal Tests

Q_l $m^3\ hr^{-1}$	GVF / %										
	5	10	20	30	40	50	60	70	80	90	95
3.6											
7						x	x	x	x	x	x
15				x	x	x	x	x	x	x	
25			x	x	x	x	x	x	x		
35		x	x	x	x	x	x				
45		x	x	x	x	x					
55		x	x	x							
63		x	x	x							
72		x	x								
90	x	x									

Table 3 - Nominal Two-phase Gas-liquid Test Matrix for Vertical Tests

Q_l $m^3\ hr^{-1}$	GVF / %								
	15	30	50	70	80	90	95	98	99.5
1.8						x	x	x	x
15			x	x	x	x	x	x	
40		x	x	x	x				
70	x	x	x						

5 RESULTS AND DISCUSSION

5.1 Test Matrices

Figures 6 and 7 below shows the test points completed. In the horizontal orientation, the flow regime primarily observed was slug flow with a few points with bubble flow. In the vertical orientation slug and churn flow were observed, with one instance of annular flow. This agrees with the observations made through the Perspex viewing section directly upstream of the tomography spool piece for both orientations.

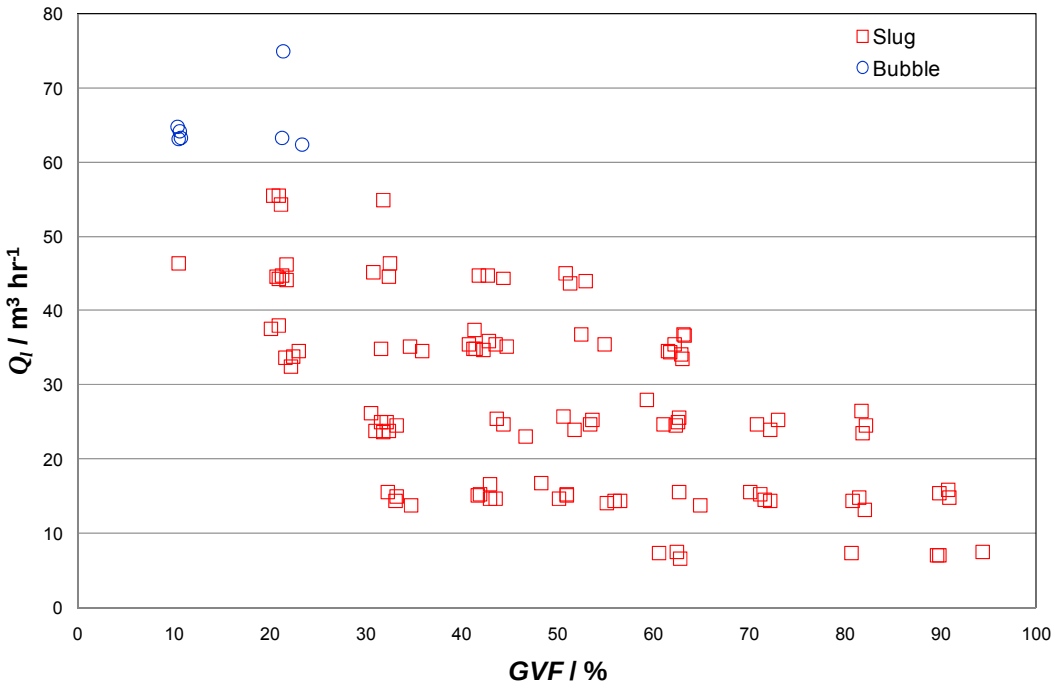

Fig. 6 - Horizontal tests completed

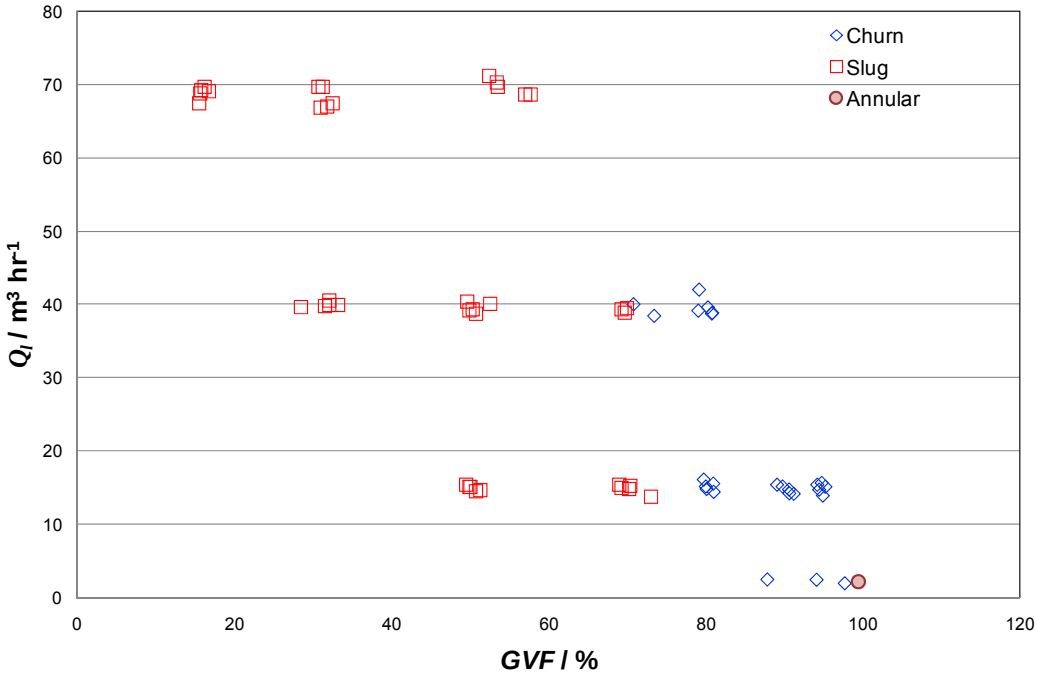

Fig. 7 - Vertical tests completed

5.2 Void Fraction Comparisons

As noted in Section 4.3, a gamma densitometer was used to record the average mixture density downstream of the tomographic spool piece. By assuming that the density recorded by the gamma densitometer is a simple line average along the gamma beam vertically down the pipe diameter, as shown in Figure 8, it is possible to calculate the height of the liquid to gas interface and hence the void fraction.

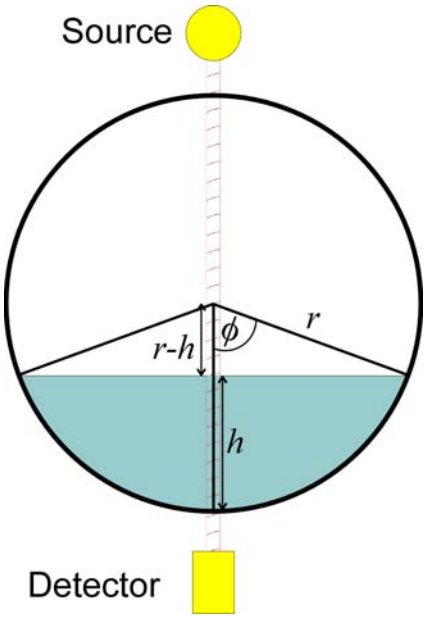

Fig. 8 - Void fraction calculation from gamma densitometer data

With reference to Figure 8, the average density recorded by the gamma densitometer will be

$$\rho_{gamma} = \frac{h}{d}\rho_{liquid} + \frac{(d-h)}{d}\rho_{gas} \qquad (2)$$

where h is the height of the interface above the bottom of a pipe of diameter d, the lower part of which is filled with a liquid of density ρ_{liquid}, above which is gas of density ρ_{gas}. Equation 2 can be rearranged to give

$$h = \frac{d\left(\rho_{gamma} - \rho_{gas}\right)}{\rho_{liquid} - \rho_{gas}} \quad . \qquad (3)$$

Application of basic trigonometry enables the area of the pipe occupied by liquid to be calculated from

$$A_{liquid} = \phi r^2 - r(r-h)\sin\phi \qquad (4)$$

and hence the void fraction, ε, can be obtained from

$$\varepsilon = 100\left(1 - A_{liquid}/A_{pipe}\right) \quad . \qquad (5)$$

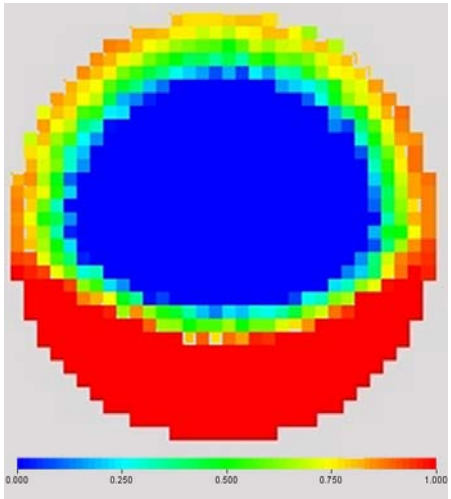

Fig. 9 - Typical ECT image

The software supplied with the dual-modality tomography system enabled the export of "relative permittivity" data from ECT images, from which true area-based void fractions can be calculated. Figure 9 shows a typical ECT image, representing one frame from a test run. The relative permittivity is 0 for an air-filled sensor and 1 for an oil-filled sensor so the mean permittivity is an estimate of the liquid hold-up.

During the test programme the logging frequency of the gamma densitometer was 5 Hz whereas the dual-modality tomography system logged at between 5 and 20 Hz, depending on the mode of operation, with most data being collected at 20 Hz.

An initial comparison of gas void fractions from the ECT data with the gas void fractions calculated using the gamma densitometer for the horizontal orientation showed that the gamma densitometer values tended to be greater as a general rule but not always. The difference appeared to be related to the flow rate of the gas and/or the gas volume fraction, as can be seen in Figures 10 and 11.

Those points where the void fraction determined by the tomography system was significantly greater than the value determined from the gamma densitometer data correspond to water-continuous conditions. The TUV NEL multiphase facility uses a brine substitute consisting of magnesium sulphate crystals ($MgSO_4.7H_2O$) dissolved in mains water. The ECT side of the dual-modality tomography system initially used a lower limit based on the permittivity of gas and an upper limit based on the permittivity of oil to distinguish the gas phase from the liquid phase. The permittivity of the brine substitute used during testing was so much greater than

that of the oil that the water can block the capacitance, so that water appears as gas on the tomogram. Initially there were issues with the brine substitute on the ERT side as well but this was rectified using a network resistance adaptor. The effects of water with high conductivities on electrical tomography systems have been investigated by Jaworski and Bolton [14].

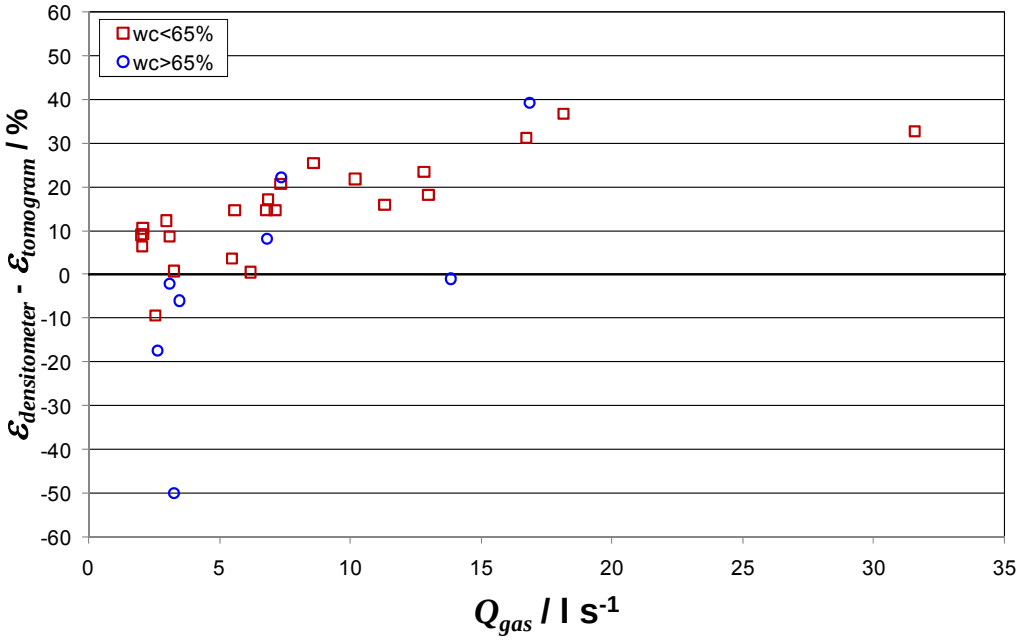

Fig. 10 - Difference in gas void fractions vs gas flow rate, horizontal orientation, initial references

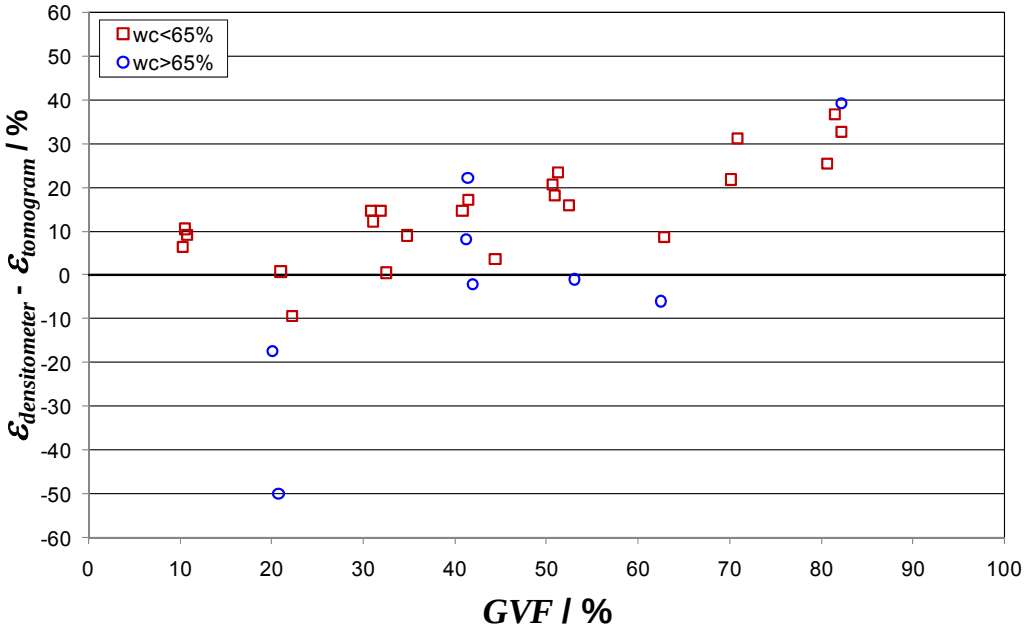

Fig. 11 - Difference in gas void fractions vs GVF, horizontal orientation, initial references

It was initially assumed that for points in the oil-continuous region, the difference could possibly be attributed to the flow regime, which is partly determined by the gas flow rate. Figures 12a and 12b show the cross-sectional view of the pipe and the stacked images respectively of slug flow taken by the ECT in horizontal orientation. The red part of the tomogram represents liquid and the blue part is the gas. The cross-sectional tomogram

image shows a curved interface between the gas and the liquid as well as some liquid hold-up at the pipe wall. This gives a larger liquid hold-up than the gamma densitometer and its single path measurement, and hence a smaller gas void fraction.

The upper part of the stacked tomogram is the image of the top half of the pipe at the centre-line, viewed from the side. This gives an indication of the frequency and size of the slugs. The lower tomogram is the image at the mid-plane of the pipe, viewed from above. These images confirm that for the flow conditions in this test the slugs are relatively regular in size and that the liquid / gas interface is curved.

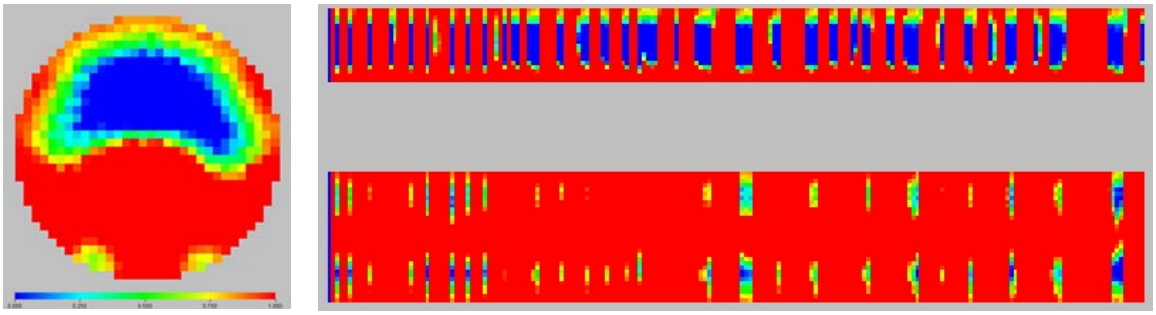

(a) (b)

Fig. 12 – Tomograms for test point FGRE310501 (horizontal orientation)

Figure 13 shows the calculated gas void fractions over a 20 second period. It would appear that the ECT shows more events, i.e. slugs, due to its faster sampling rate of 20Hz compared to the 5Hz sampling rate of the gamma densitometer. Whilst it may be thought that this would lead to the ECT-based void fraction being higher, it appeared to be the case that the ECT was detecting more of the liquid, including the significant amounts accounted for by the curved interface, than detected by the gamma densitometer.

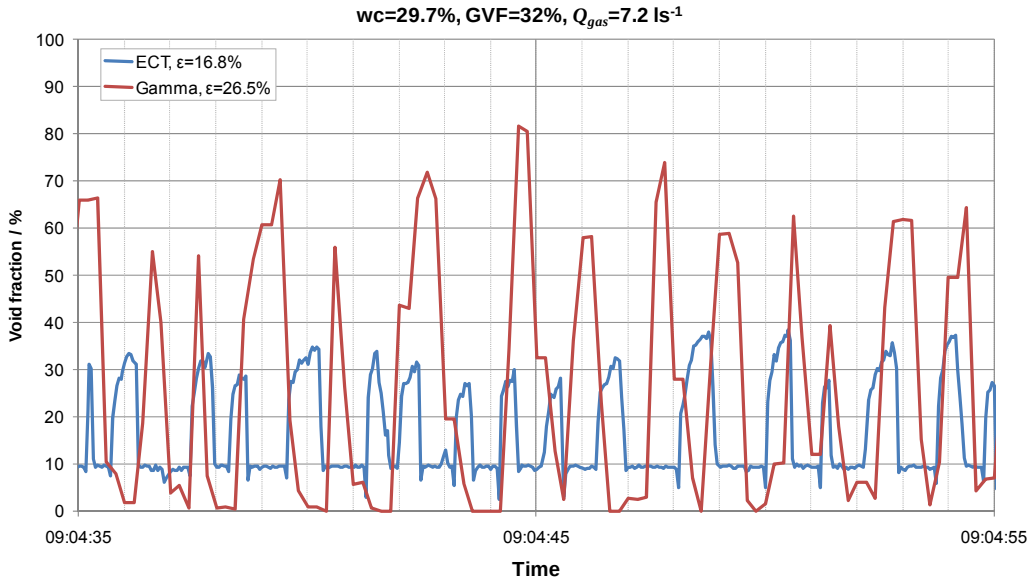

Fig. 13 - ECT and gamma void fractions for test point FGRE310501 (horizontal orientation)

Figures 14a and 14b show the cross-sectional view and stacked images for a test point with much higher gas flow rate and gas volume fraction than the previous example in horizontal orientation, representing a more extreme instance of slug flow.

As can be seen in Figure 14a, the liquid / gas interface is extremely curved, with significant liquid hold-up on the upper part of the pipe. Although the plot of the gas void fractions for this test point over a 20 second period (Figure 15) shows that the ECT is detecting even more

events (slugs) than the gamma densitometer, the significant amounts of liquid hold-up and curved interface contribute to the ECT-derived void fraction being smaller than that derived from the gamma densitometer data. Furthermore, the conditions in this test resulted in relatively small, fast-moving liquid-filled regions of the pipe between the large gas slugs. Previous (qualitative) experiments with the gamma densitometer using a liquid-filled phantom indicated that that faster the phantom (slug) was moved through the gamma densitometer beam, the less it was recorded [15]. For the conditions pertaining in this test it appeared that the gamma densitometer was not seeing all of the liquid and hence the calculated void fractions were higher than those derived from the ECT data.

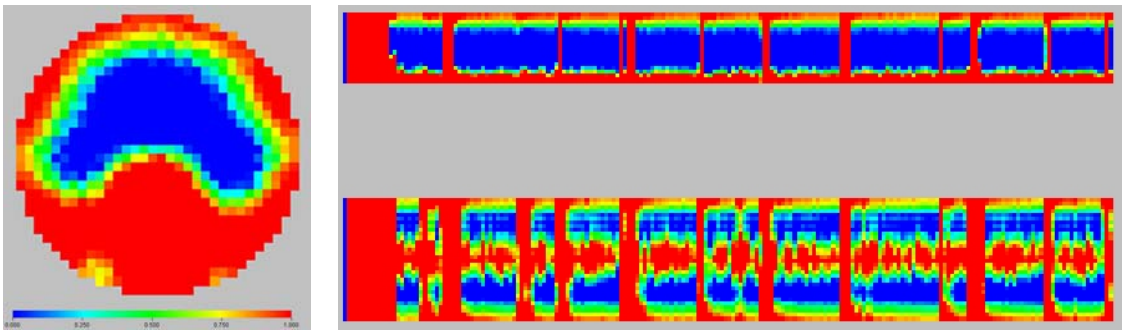

(a) (b)

Fig. 14 – Tomograms for test point FGRE310512 (horizontal orientation)

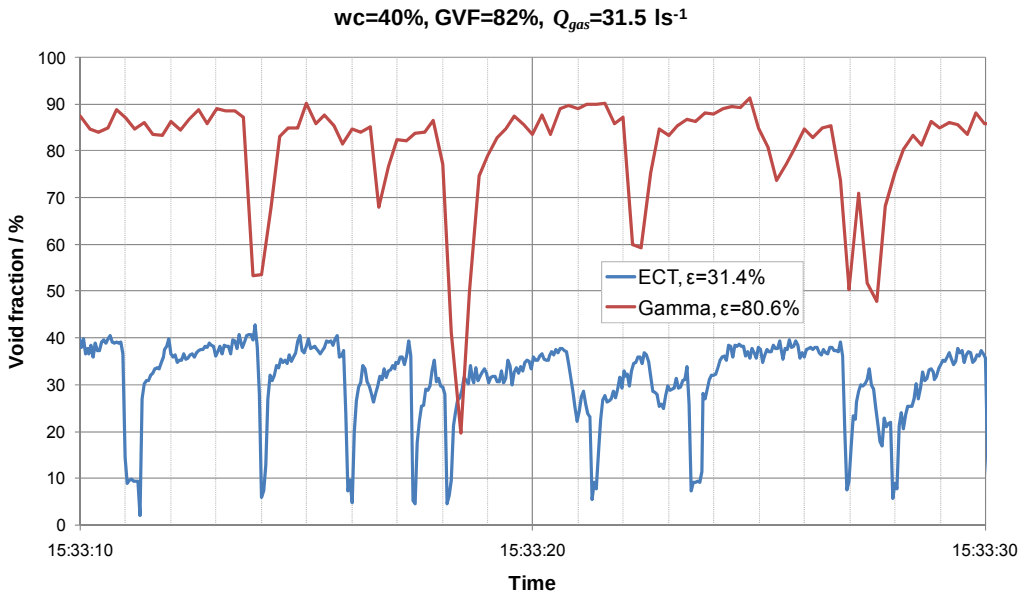

Fig. 15 - ECT and gamma void fractions for test point FGRE310512 (horizontal orientation)

A simple analysis was carried out to ascertain whether the shape of the interface and liquid hold-up at the wall could lead to the observed differences between the gamma densitometer- and ECT-derived void fractions.

Figure 16a represents a pipe filled with 50% liquid and 50% gas, on a 32 x 32 grid, corresponding to the pixel-based approach as used by the data analysis system in the ECT part of the dual-modality tomography system. Using a line-based void fraction calculation analogous to that used for the gamma densitometer gives a gas void fraction of 50.5%. An area based void fraction calculation of the type used by the tomography system gives an answer of 50%. The slight difference in answers is due to the difference in the calculated area of the pipe when treated as a circle of radius 16 (804) or by counting pixels (812).

Figure 16b represents a pipe filled mostly with gas, the line-based and area-based calculations giving answers of 84.0% and 83.7% respectively. Again the slight difference is due to the differences in the area calculations.

When the interface is a straight line, the line-based and area-based void fraction calculations tend to agree with each other. However, looking at an example which is more representative of Figures 12a and 14a with the curved interface and liquid hold-up at the pipe wall, the difference in calculation methods becomes more apparent. The image in Figure 17 gives a line based void fraction of 84.0% and an area based void fraction of 71.9%.

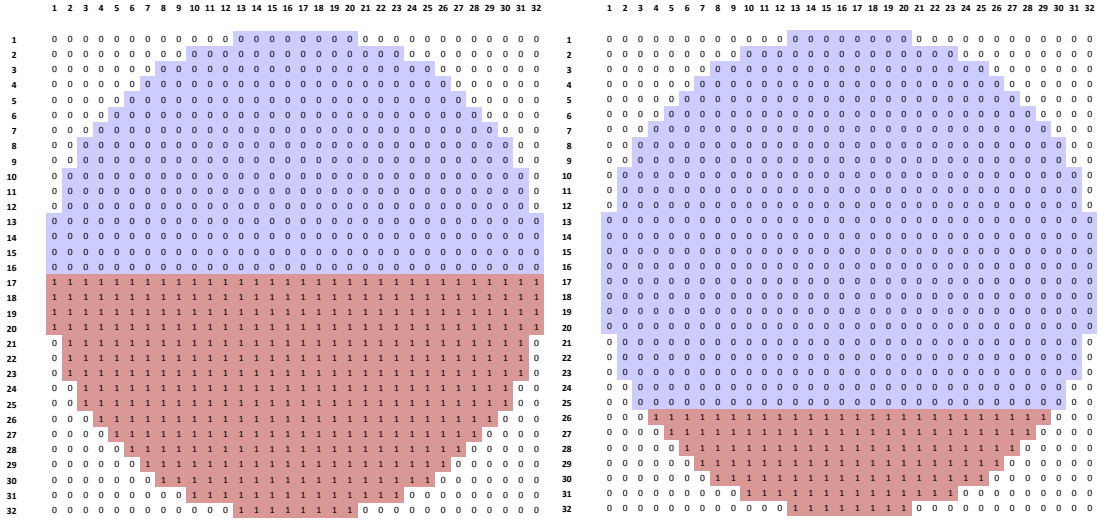

(a) (b)

Fig. 16 - Pixel representation of a pipe filled with gas and liquid - straight interface

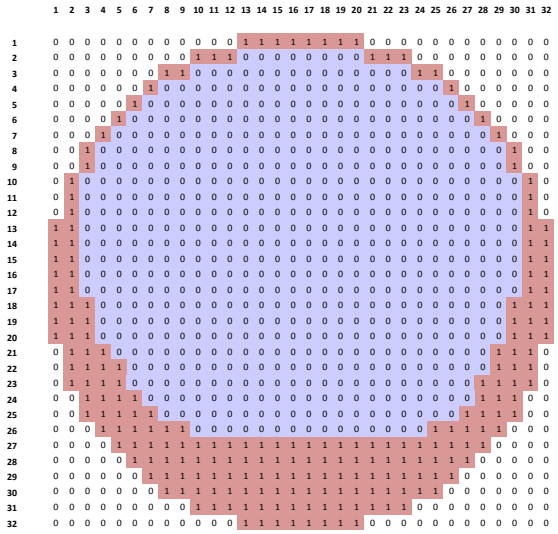

Fig. 17 - Pixel representation of a mainly gas-filled pipe with curved interface

As the line based method assumes a linear interface it is possible it has a tendency to under-estimate the liquid hold-up which in turn means the gas void fraction would be over-estimated. As the curvature of the interface increases with higher gas flow rates this is potentially an explanation for the differences observed in the test results.

However, this effect is not sufficient to explain the observed differences between the gamma densitometer- and ECT-derived void fractions. The tomography system supplier therefore re-examined the tomogram data processing method.

As noted above, the ECT side of the dual-modality tomography system processes the raw data using reference values. Initially a lower limit based on the permittivity of gas and an upper limit based on the permittivity of oil were used to distinguish the gas phase from the liquid phase. However, for the majority of flow conditions in horizontal orientation in the TUV NEL Multiphase Flow Facility, the oil and water effectively form a pseudo single phase with mixed fluid properties. Using the permittivity of pure oil as the upper reference limit may therefore lead to over-estimation of the liquid content (and hence underestimation of the void fraction) as even small amounts of water will significantly increase the measured permittivity, taking the value above the oil-based upper limit and hence appearing as all “liquid”. The tomography system supplier therefore suggested re-processing the data using theoretical mixed oil-water references, based on the known water cuts for each test point, since the permittivity of a homogenised two-component fluid mixture can be well approximated by a simple mole fraction average of the component permittivities.

Figures 18 shows the data from the oil-continuous horizontal orientation tests and Figure 19 shows the data from the vertical orientation tests re-processed using theoretical mixed oil-water references. However, with this approach it appears that the tomography data are now generally over-predicting void fractions compared with the values derived from the gamma densitometer data.

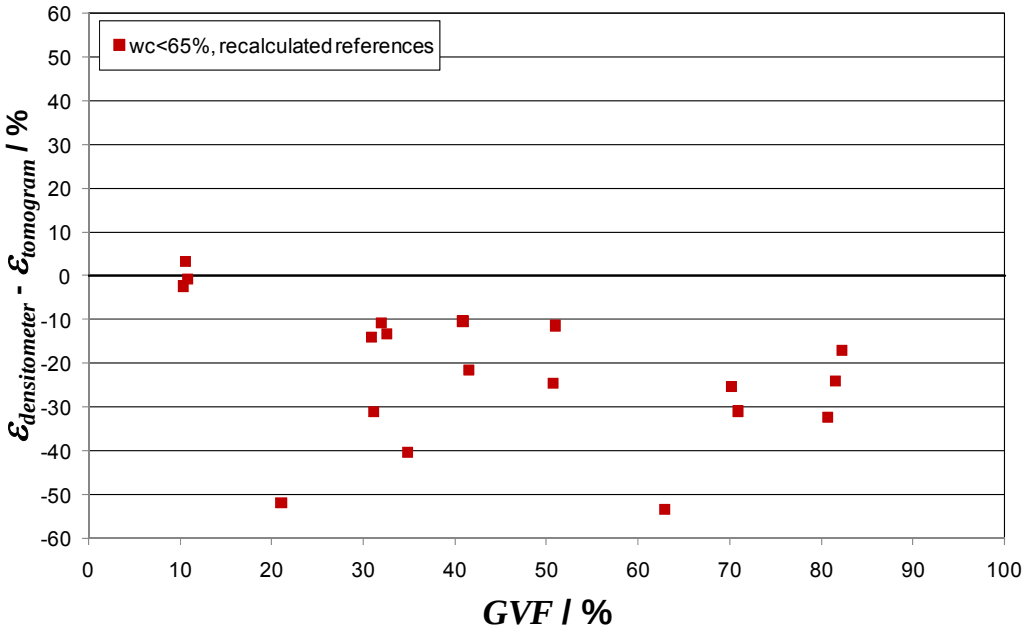

Fig. 18 - Difference in gas void fractions vs GVF, horizontal orientation, recalculated references

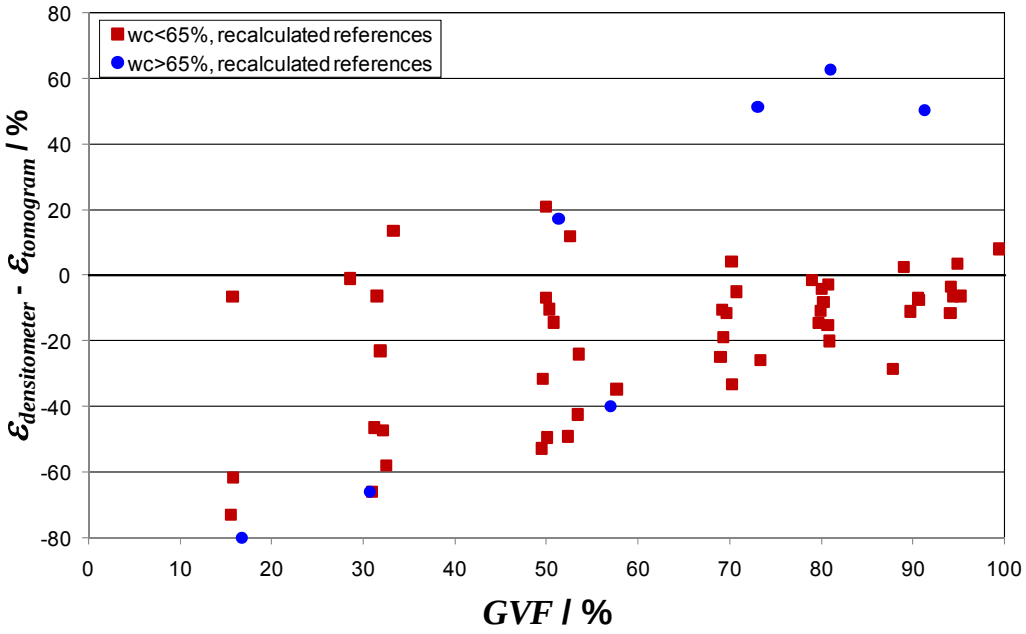

Fig. 19 - Difference in gas void fractions vs GVF, vertical orientation, recalculated references

Following further discussion with the tomography system supplier, a revised method of using experimentally determined mixed fluid-phase references was developed. So far, only a limited amount of data has been reprocessed using this approach but the results look promising, as shown in Figure 20.

5.3 Discussion

So far, efforts have been focussed on validating the ECT part of the dual-modality system. Further analysis will be carried out using the data collected by the ERT side. The images produced by the ERT will give additional visualisation information with regards to the oil and water distribution in the liquid phase.

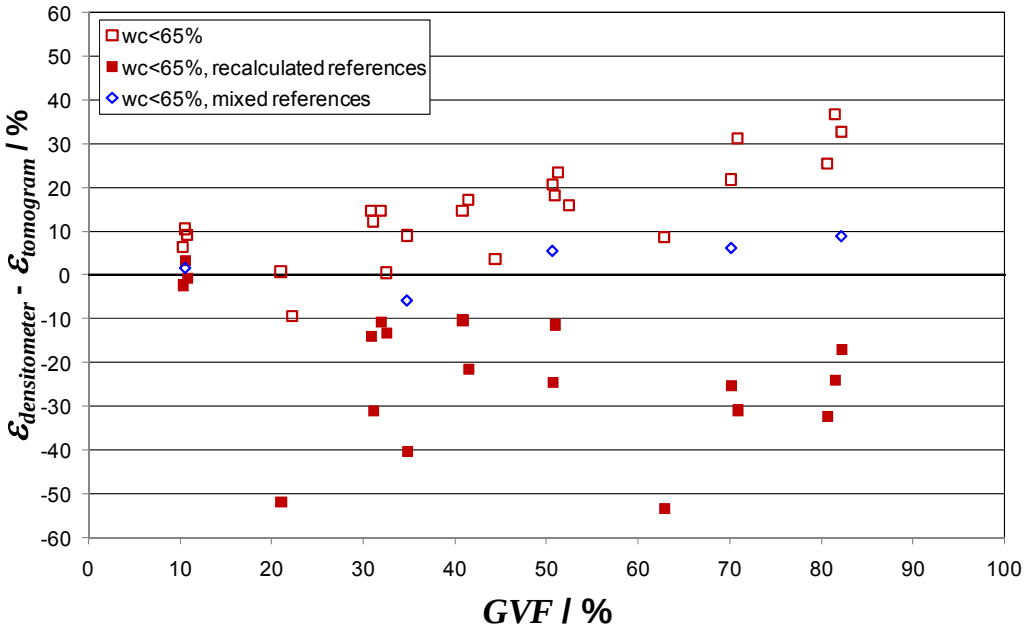

Fig. 20 - Effect of reference on difference in gas void fractions vs GVF, horizontal orientation

Whilst results so far show potential there is still the issue of data fusion. Being able to combine the ECT and ERT images in a single tomogram would make visualisation of complex flows easier.

The main issues encountered when the tomography system was installed in the multiphase test facility were the effect of the water salinity on the dual-modality system, and the need for good references.

Many tomography systems based on electrical properties are in use in universities around the world. Those that have tomography systems based on electrical properties use distilled water and in some cases triple distilled water. As noted previously, the TUV NEL multiphase facility uses a brine substitute consisting of magnesium sulphate crystals ($MgSO_4.7H_2O$) dissolved in mains water and appropriate references must therefore be used

The dual-modality tomography system relies upon the user to take good reference measurements, i.e. single phase water, oil, and gas, or other appropriate references. The better the references used, the better the data collected during testing. This is very similar to many multiphase flow meters in that their performance is heavily reliant on having good fluid property data. It is possible though to post process data with references taken after testing.

Tomography systems still appear to be aimed at more research-based work and as such offer considerable flexibility. Customisation of the user interface is generally required to simplify operation for more industrial applications.

6 CONCLUSIONS

The purpose of this project was to gain a better understanding of the TUV NEL multiphase test facility by using a dual-modality tomography system to visualise the complex flows. It must be stressed that the tomography system was to be used to characterise the flow

patterns and not for flow measurement purposes. However, at its current state of development, the dual-modality tomography system evaluated as part of this project was not suitable for this application. TUV NEL has therefore decided not to install the system on the multiphase flow facility at present.

So far, testing has shown that there can be significant differences between the void fractions calculated using the ECT data and the gamma densitometer data, depending on the reference values used to process the raw data from the tomography system. By using appropriate references, it appears to be possible to obtain good agreement between the two techniques, at least over significant parts of the flow regimes.

Whilst it may be argued that comparing void fractions derived from an area-based technique such as tomography with those derived from a line-based technique such as gamma densitometry is unrealistic (due to the effects of a curved liquid / gas interface plus liquid hold-up not detected by the gamma beam), most commercially-available multiphase flowmeters rely on gamma densitometers to provide phase split information and hence there is a perception that gamma densitometer-derived phase information will always be correct. This may not always be the case. At the throat of a Venturi under ideal conditions, the fluid may be sufficiently well mixed that the phase splits derived from a line-based gamma densitometer will be close to the true phase splits. However, this will not be the case in highly chaotic flow situations such as slug and churn flow. In principle therefore, validation of any particular tomographic technique could strictly only be undertaken using another tomographic technique, which itself would have had to be validated.

Despite the difficulties alluded to above, electrical-based tomographic techniques have the potential to provide useful information on phase splits and flow structures in multiphase flows. In addition, the use of modelling as a predictive tool in complex flows is well established, and the ability to visualise a real flow stream would have a major impact on the validation of modelling software. It would allow users to have confidence in the use of codes in more challenging flow systems, bringing benefits to many industrial sectors.

7 ACKNOWLEDGEMENTS

The work described in this paper was undertaken by TUV NEL Ltd as part of a National Measurement System project entitled ‘Complex flow characterization: Assessment of technologies and development of capability’, under the National Measurement Office’s Engineering & Flow Programme.

The extensive support of the supplier of the dual-modality tomography system (ITS Ltd) is also gratefully acknowledged.

The authors also wish to thank their colleagues at TUV NEL who contributed to the experimental programme, in particular Richard Harvey.

8 NOTATION

A	Pipe cross sectional area	m^2
C	Capacitance	Farad
d	Pipe ID	m
h	Liquid interface height	m
K	Sensor geometry constant	$Farad^{-1}$
r	Pipe radius	m

Greek symbols

ε_m	Average fluid dielectric within sensing volume	-
ε	Void fraction	-
ϕ	Angle	rad

Subscripts

gas	gas phase
gamma	gamma densitometer
liquid	liquid phase

8 REFERENCES

[1] A. ROSS. Background and Evaluation of Tomographic Techniques. Report No: 2009/20 produced for DIUS; TUV NEL Ltd, East Kilbride, January 2009.

[2] A. ROSS. Evaluation of Available Tomography Systems and their Suitability for TUV NEL Facilities. Report No: 2009/21 produced for DIUS; TUV NEL Ltd, East Kilbride, January 2009.

[3] I. ISMAIL, J.C. GAMIO, S.F.A. BUKHARI and W.Q. YANG. Tomography for Multiphase Flow Measurement in the Oil Industry. *Flow Measurement and Instrumentation*, **16**, 145-155, 2005.

[4] HANDBOOK OF MULTIPHASE FLOW METERING. Revision 2, March 2005. The Norwegian Society for Oil and Gas Measurement, The Norwegian Society of Chartered Technical and Scientific Professionals. Page30

[5] M.S. BECK and R.A. WILLIAMS. Process Tomography: A European Innovation and its Applications. *Meas. Sci. Technol*. **7**, 215-224, 1996.

[6] M. WANG, T.F. JONES and R.A. WILLIAMS. Visualisation of asymmetric solids distribution in horizontal swirling flows using electrical resistance tomography. *Trans IChemE*, **81**, Part A, 854-861, 2003.

[7] R. GIGUÉRE, L. FRADETTE, D. MIGNON and P.A. TANGUY. Characterisation of slurry flow regime transitions by ERT. *Chemical Engineering Research and Design*,. **86**, 989-996, 2008.

[8] A.J. JAWORSKI and T. DYAKOWSKI. Application of Electrical Capacitance Tomography for Measurement of Gas-Solids Flow Characteristics in a Pneumatic Conveying System. *Meas. Sci. Technol*, **12**(8) 1109-1119, 2001.

[9] S.J. WANG, D. GELDHART, M.S. BECK and T. DYAKOWSKI. A Behaviour of a Catalyst Powder Flowing Down in a Dipleg. *Chem. Eng. Journal*, **77**(1-2), 51-56, April 2000.

[10] J.C. GAMIO, J. CASTRO, L. RIVERA, J. ALAMILLA, F. GARCIA-NOCETTI and L. AGUILAR. Visualisation of Gas-Oil Two-Phase Flows in Pressurised Pipes Using Electrical Capacitance Tomography. *Flow Measurement and Instrumentation*, **16**(2-3), Pages 129-134, April-June 2005.

[11] T. GROTH, M. REICHWAGE, D. MEWES and A. LUKE. Effects of Dissolving and Degassing Phenomena on Multiphase Oil and Gas Boosting. Proceedings of 14th International Conference on Multiphase Production Technology, Cannes, France:17-19 June 2009.

[12] E.A. HAMMER. Three-component flow measurement in oil/gas/water mixtures using capacitance transducers. Ph.D. Thesis, University of Manchester, 1983.

[13] B.S. HOYLE, X. JIA, F.J.W. PODD, H.I. SCHLABERG, H.S. TAN, M. WANG, R.M. WEST, R.A. WILLIAMS and T.A. YORK. Design and application of a multi-modal process tomography system. *Measurement Science and Technology*, **12**, 1157-1165.

[14] A.J. JAWORSKI and G.T. BOLTON. The design of an electrical capacitance tomography sensor for use with Media of High Dielectric Permittivity. *Meas. Sci. Technol.* **11**, 743–757, 2000.

[15] R. HARVEY. Personal communication, TUV NEL, 2009.